Pergamon

Geochimica et Cosmochimica Acta, Vol. 66, No. 3, pp. 361–381, 2002

0016-7037/02 $22.00 + .00

PII S0016-7037(01)00685-8

The oxygen geochemical cycle: Dynamics and stability

ANTONIO C. LASAGA[1] and HIROSHI OHMOTO[2,*]

[1]Department of Geology and Geophysics, Yale University, New Haven, Connecticut 06520, USA
[2]Astrobiology Research Center and Department of Geosciences, The Pennsylvania State University, University Park, Pennsylvania 16802, USA

(*Received January* 26, 2001; *accepted May* 17, 2001)

Abstract—The first and possibly only major rise of atmospheric oxygen, from $p_{O_2} \leq 0.1\%$ PAL (the present atmospheric level) to $p_{O_2} \geq 10\%$ PAL, appears to have occurred sometime before 2 Ga ago, although the exact time of and the cause(s) for the rise have been hotly debated. Equally important questions on the atmospheric oxygen concern its stability, especially the mechanisms regulating the atmospheric p_{O_2} level and the causes and magnitude of p_{O_2} variations since the first major rise of atmospheric oxygen. Previous efforts to model the p_{O_2} variation during the Phanerozoic time have typically relied on secondary information, such as the carbon and sulfur isotopic records of sedimentary rocks, and on simple dynamics of the geochemical cycles of O, C, S, and P based on box-type models. As a result, many kinetic questions about the variation and stability of atmospheric oxygen could not have been answered. Here we quantitatively evaluate the dynamics and stability of atmospheric O_2 and CO_2, using recent experimental data, field observations, and a new model for the C–O coupled geochemical cycles. We examine the change with time in the fluxes of various compounds (O_2, CO_2, phosphate, organic C, carbonate C, C-bearing reduced volcanic gases, and C-free reduced volcanic gases) among the various reservoirs (atmosphere, soil, surface ocean, deep ocean, the lower crust and mantle, and upper crust) under a variety of scenarios. Our model does not assume steady-state fluxes for any of the reservoirs. Rather, the model incorporates the kinetic experimental data on oxidation of coal, a proxy for kerogen, the dynamics of soil formation and erosion, the kinetics of decomposition of organic matter in the Oceans by aerobic and anaerobic bacteria, the equilibrium ocean–atmosphere carbonate model, the observed relationships among the organic burial flux, dissolved O_2 content of deep ocean, and sedimentation rates, and the three-box model ocean. The important parameters that strongly influence the dynamics of atmospheric O_2, are found to be (a) the total area of soil formation on Earth; (b) the average soil depth; (c) the average rate of physical erosion of soils, which is linked to the average rate of accumulation of clastic sediments in the oceans; (d) the composition and flux of volcanic gas; and (e) the level of atmospheric CO_2. We develop kinetic equations linking these parameters to the production and consumption fluxes of atmospheric oxygen and also to stable p_{O_2} values. Considering the likely ranges of variations in these parameters in geologic history, we suggest that the atmospheric p_{O_2} level is likely to have stayed within a very narrow range of 0.6–2 PAL and that the entire ocean, except for local euxinic basins, is likely to have been basically oxygenated since the first major rise of atmospheric oxygen more than 2 Ga ago. *Copyright © 2002 Elsevier Science Ltd*

1. INTRODUCTION

For the last several decades, there has been much debate concerning the evolutionary history of atmospheric oxygen. Opinions vary as to when the first oxygen-producing photosynthetic organisms, probably cyanobacteria, appeared on Earth; when the atmospheric O_2 level first rose to ~5% of the present atmospheric level (PAL), which is the minimum value needed to sustain the activity of most eukaryotic microbes (Jahnke and Klein, 1979); and when the p_{O_2} rose to ~50% PAL which is the minimum value required by animals (Knoll, 1992). For example, some microfossils and stromatolites in ~3.4 Ga sedimentary rocks in the Pilbara district of Australia and in the Barberton district of South Africa have been linked to cyanobacteria (e.g., Schopf, 1994), but they may be related to nonoxygenic photoautotrophs or even chemoautotrophs. Holland (e.g., 1994) suggests a dramatic rise of p_{O_2} from <0.1% PAL to >15% PAL at about 2 Ga ago, and Knoll (1992) suggests another rise of p_{O_2} to >50% PAL as a cause of the Cambrian Biological Evolution ~600 Ma ago. In contrast, Ohmoto (1997) suggests that the p_{O_2} very quickly rose to the present atmospheric level more than 3.5 Ga ago and remained within ± 50% of PAL since then.

Various investigators (e.g., Garrels and Lerman, 1984; Kump and Garrels, 1986; Lasaga, 1989; Berner et al., 2000; Berner, 2001) have modeled the variation of atmospheric p_{O_2} during the Phanerozoic time based on carbon and sulfur isotopic records of sedimentary rocks and on simple box-type models of the geochemical cycles of oxygen, carbon, and sulfur. Their studies suggest that the atmospheric p_{O_2} has fluctuated within a very narrow range of ~0.5 to ~2 PAL during the Phanerozoic. Since the appearance of vascular plants on land ~400 M yr ago, the maximum p_{O_2} may have been limited to ~1.4 PAL by forest fires (Watson et al., 1978; Kump, 1988).

If the atmospheric p_{O_2} level drops below ~0.5 PAL, the ocean below the photic zone is likely to become anoxic (e.g., Sarmiento, 1992), causing major extinction of marine organisms; the ozone shield in the atmosphere will also become considerably thinner, causing major extinction of land-based organisms. Thus, the following questions become important: "Why has the p_{O_2} level always stayed above ~0.5 PAL during the Phanerozoic?", "Has the p_{O_2} level ever dropped below ~0.5 PAL (or ~0.1 PAL) since the first rise of p_{O_2} from <0.001 PAL

* Author to whom correspondence should be addressed (ohmoto@geosc.psu.edu)

to >0.5 PAL, regardless of whether the first rise occurred ~1.0 G yr, ~2.0 G yr or earlier?" and "What was the maximum p_{O_2} level prior to the appearance of vascular plants?" These questions can be answered only when the mechanisms regulating the atmospheric p_{O_2} level are understood.

Holland first proposed in 1973 the dependence on p_{O_2} of the O_2 consumption flux by soil (F_{s,O_2}) and of the O_2 production flux by organic carbon burial ($F_{b,org}$) as the major negative feedback mechanisms for regulating the atmospheric oxygen level. However, recently this idea has not been pursued for the following reasons: (1) The oxidation rates of reducing compounds in rocks have been thought to be so fast that all the reducing compounds in soils are oxidized. Therefore, the F_{s,O_2} value depends only on the erosion (exposure) rate and not on the atmospheric p_{O_2} (e.g., Berner, 1999); (2) from an analysis of geochemical data on modern marine sediments, Betts and Holland (1991) recognized only a very weak dependency of $F_{b,org}$ on the dissolved O_2 content of seawater. Subsequently, most of the current models (Holland, 1984; Kump, 1988; Van Cappellen and Ingall, 1996; Lenton and Watson, 2000) for negative-feedback mechanisms involve changes in the burial flux of organic carbon ($F_{b,org}$) often modulated by changes in biological productivity and the cycling of phosphorus. Here we report that our analyses of recent experimental data on the oxidation kinetics of coal (Chang and Berner, 1999) and of geochemical data on marine sediments (e.g., Betts and Holland, 1991; Arthur et al., 1994) lead to a suggestion that the two negative-feedback mechanisms initially proposed by Holland (1973; 1978) are indeed the most likely mechanisms for effectively regulating the atmospheric p_{O_2} around the present level.

2. BASIC CONCEPTS

2.1. Holland's Semiquantitative Approach

The overall control of p_{O_2} in the atmosphere depends ultimately on the balance between the production fluxes of O_2 and the consumption fluxes of O_2 (see Figs. 1 and 2). Holland (1973; 1978; 1984) was the first to (semi)quantitatively evaluate the interplay between these fluxes (Fig. 2). That is,

$$\frac{dM_{O_2}}{dt} = F_{prod,O_2} - F_{sink,O_2} \quad (1)$$

in which dM_{O_2}/dt refers to the change in the total O_2 content of the atmosphere + ocean system, F_{prod,O_2} the O_2 production flux, and F_{sink,O_2} the consumption flux of O_2.

Atmospheric O_2 has been generated by O_2-producing photosynthetic organisms (mostly cyanobacteria) utilizing CO_2 and H_2O through the following simplified biochemical reaction:

$$CO_2 + H_2O \Leftrightarrow CH_2O + O_2 \quad (2)$$

in which CH_2O refers to organic matter. The current production rate of O_2 (and organic matter) by photosynthesis is $\sim 7 \times 10^{15}$ moles/yr each by terrestrial and by marine organisms (Sundquist, 1985). Because the total amount of O_2 in the atmosphere is 38×10^{18} moles (see Table 1), we may consider that the residence time of atmospheric O_2 based on the biosphere is 38×10^{18} moles/(14×10^{15} moles/yr) or ~3000 years, and that the p_{O_2} level within a time scale of ~3000 yrs is influenced by the variation in the biological activity on land as well as in the oceans. However, on a time scale of more than 3000 yrs, essentially all the O_2 and organic matter produced by organisms are converted back to CO_2 and H_2O through the reverse of reaction (2), as long as the products are exposed to the atmosphere. Then, there will be no net change in the atmospheric content of O_2. For this reason, the biological activity on land does not affect the long-term (>3000 yrs) content of O_2 in the atmosphere.

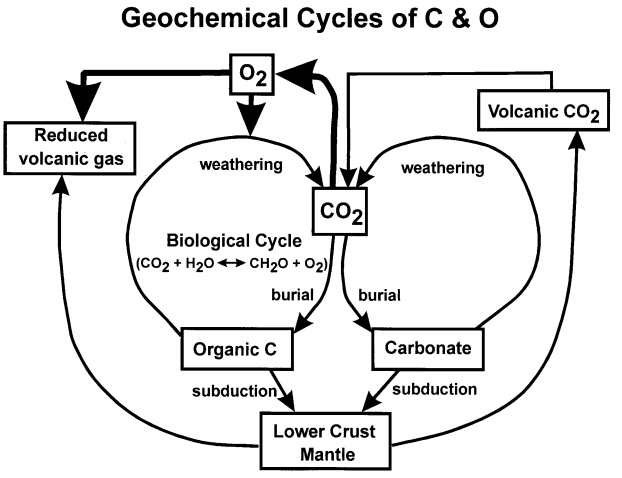

Fig. 1. Schematic illustration of the carbon and oxygen geochemical cycles. Note that the long-term production rate of atmospheric O_2 equals the burial rate of organic C in sediments, and that the atmospheric O_2 is consumed by reduced volcanic gas and by rock weathering.

Accumulation (production) of atmospheric O_2, on a time scale of more than 3000 years, occurs when some of the organic matter generated in the ocean (and lakes) is buried in sediments, preventing the reverse of reaction (2) from taking place. Since the burial of 1 mole of organic carbon generates 1 mole of O_2, the long term (>3000 years) production flux of O_2

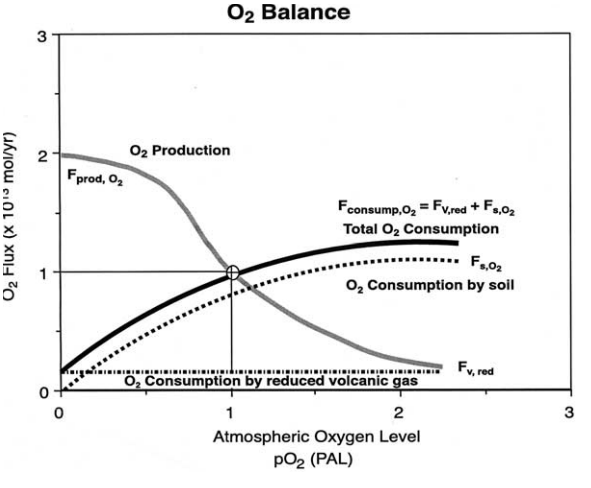

Fig. 2. Schematic diagram illustrating the relationship among the oxygen content of the atmosphere, the rate of oxygen production, F_{prod,O_2}, and the rate of oxygen consumption, $F_{consump,O_2}$ (modified from Figs. 6–12 of Holland, 1978). ⊕ marks the steady state value today.

Table 1. System parameters.

Symbol	Explanation	Present day value
		(m^2)
A_{land}	Total area of soil-forming land	$A^0_{land} = 1.5 \times 10^{14}$
$A_{s,org}$	Total surface area of organic matter in soil reservoir	$A^0_{s,org} = 0.29 \times 10^{18}$
$\bar{A}_{org}$	Specific surface area of organic matter in rocks	$\bar{A}_{org} = 0.12$ m^2/g
		(cm/yr)
dh/dt	Soil erosion rate	$dh/dt^0 = 0.005$
		$\times 10^{12}$ moles/K yr
$F_{b,org}$	Burial flux of organic carbon	$F^0_{b,org} = 10{,}000$
$F_{b,carb}$	Burial flux of carbonate carbon	$F^0_{b,carb} = 40{,}000$
$F_{b,P}$	Burial flux of phosphate	
$F_{det,sed}$	Flux of detrital sediments to ocean	$F^0_{det,sed} = 1.5 \times 10^{19}$ g/K yr
$F_{det,org}$	Flux of detrital organic matter to ocean	$F^0_{det,org} = 3{,}500$
F_{net,O_2}	Net flux of O_2	$F^0_{net,O_2} \sim 0$
$F_{net\ prod,O_2}$	Net production flux of O_2	$F^0_{net\ prod,O_2} = 7500$
$F_{prod,org}$	Production flux of organic carbon	$F^0_{prod,org} = 3.3 \times 10^6$
F_{prod,O_2}	Production flux of O_2	$F^0_{prod,O_2} = 10{,}000$
F_{s,O_2}	Consumption flux of O_2 by soils	$F^0_{s,O_2} = 7500$
F_{sink,O_2}	Total consumption flux of O_2	$F^0_{sink,O_2} = 10{,}000$
$F_{sub,org}$	Subduction flux of organic carbon	$F^0_{sub,org} = 1500$
$F_{sub,carb}$	Subduction flux of carbonate carbon	$F^0_{sub,carb} = 6{,}000$
F_{v,CO_2}	Volcanic flux of CO_2	$F^0_{v,CO_2} = 6000$
$F_{v,redC}$	Volcanic flux of reduced C (CH_4, CO)	$F^0_{v,redC} = 1500$
$F_{v,redH}$	Volcanic flux of other reduced gases (H_2, H_2S, SO_2)	$F^0_{v,redH} = 1000$
F_{v,O_2}	Consumption flux of O_2 by volcanic gases	$F^0_{v,O_2} = 2500$
$F_{w,org}$	Weathering flux of organic carbon	$F^0_{w,org} = 7500$
$F_{w,carb}$	Weathering flux of carbonate carbon	$F^0_{w,carb} = 34{,}000$
$F_{w,sil}$	Weathering flux of silicates	$F^0_{w,sil} = 6000$
$F_{w,P}$	Weathering flux of phosphate	
γ	Nonorganic fraction of burial flux of phosphate	$\gamma^0 \sim 0.2$
β	C/P atomic ratio in sediments	
α_{conv}	Conversion factor from rock to soil	$\alpha^0_{conv} \sim 1.4$
k_+	Rate constant for oxidation of coal	0.063 moles C/m^2/K yr
K_{O_2}	Michaelis–Menten parameter for organic decomposition	20 μM
L_s	Average soil depth	3 m
		$\times 10^{12}$ moles
$M_{\Sigma CO_2}$	Total amount of CO_2 and aqueous carbonate in the atmosphere and ocean	$M^0_{\Sigma CO_2} = 4 \times 10^6$
M_{O_2}	Total amount of O_2 in the atmosphere and ocean	$M^0_{O_2} = 38 \times 10^6$
M_{org}	Total amount of organic carbon in the crust	$M^0_{org} = 1.25 \times 10^9$
M_{carb}	Total amount of carbonate carbon in the crust	$M^0_{carb} = 5.0 \times 10^9$
$M_{s,org}$	Total amount of organic carbon in soils	$M^0_{s,org} = 0.2 \times 10^6$
$[O_2]_d$	Conc. of dissolved O_2 in deep ocean water	$[O_2]^0_d = 340$ μM
$[O_2]_h$	Conc. of dissolved O_2 in high-latitude surface ocean	$[O_2]^0_h = 172$ μM
$[PO_4^{3-}]_d$	Conc. of dissolved PO_4^{3-} in deep ocean water	$[PO_4^{3-}]^0_d = 2.2$ μM
$[PO_4^{3-}]_h$	Conc. of dissolved PO_4^{3-} in high-latitude surface ocean	$[PO_4^{3-}]^0_h = 1.2$ μM
		(g/cm^3)
ρ_{rock}	Specific density of rock in the crust	2.5
ρ_{soil}	Specific density of soil	2.0
		(wt. %)
$W_{r,org}$	Average content of organic carbon in weathering rock	$W^0_{r,org} = 0.45$
$W_{s,org}$	Average content of organic carbon in soil	$W^0_{s,org} = 0.28$
$W_{sed,org}$	Average content of organic carbon in new sediments	$W^0_{sed,org} = 0.61$
ξ	Burial efficiency of organic matter	$\xi^0 = 0.003$

becomes identical to the burial flux of new organic matter in sediments, $F_{b,org}$. That is,

$$F_{prod,O_2} = F_{b,org} \quad (3)$$

Holland (1978; 1984) estimates the present burial flux of new organic matter to be 10^{13} moles C/yr (or $10{,}000 \times 10^{12}$ moles/K yr). In addition, detrital fossil organic carbon from erosion of soils on land can be deposited in marine sediments. This burial does not contribute to the net production of oxygen but will be discussed later in the paper in estimating the total organic content of sediments.

Consumption of the atmospheric O_2 has been carried out primarily by two processes (Figs. 1 and 2): one is the oxidation of reduced volcanic gases (e.g., H_2, CO, H_2S), F_{v,O_2}, and the other is the oxidation of reduced compounds in rocks (organic C, sulfide S, and FeO) during weathering and soil formation, F_{s,O_2}. Therefore,

$$F_{sink,O_2} = F_{v,O_2} + F_{s,O_2} \quad (4)$$

Because the kinetics of photochemical oxidation are very fast (e.g., Kasting, 1987), the overall rate of oxygen consumption by reduced volcanic gases is completely determined by the flux of reduced gases into the atmosphere–ocean system, $F_{v,red}$, and independent of the atmospheric oxygen content [see horizontal line for F_{v,O_2} ($= F_{v,red}$) in Fig. 2].

The oxidation of reduced components in rocks exposed to subaerial weathering, F_{s,O_2}, makes up the dominant component of the total consumption flux of oxygen, shown by the dotted curve in Fig. 2. F_{s,O_2} is the center of our attention in the next section. In general, it is expected that the F_{s,O_2} value would increase with increasing p_{O_2}. However, at very large p_{O_2} values, the oxidation rate would be fast enough that other factors, such as rock exposure, would be rate limiting and the F_{s,O_2} value is expected to level out at high p_{O_2} (see Fig. 2).

Holland (1978) estimates the present values of F_{v,O_2} and F_{s,O_2} to be $(3000 \pm 1000) \times 10^{12}$ moles/K yr and $(13{,}000 \pm 3000) \times 10^{12}$ moles/K yr, respectively. That is, about 20% of the O_2 consumption is due to reduced volcanic gas and about 80% due to rock weathering. Because the calculated total O_2 consumption value $(16{,}000 \pm 4000) \times 10^{12}$ moles/K yr, is close to the estimated value for the O_2 production, $10{,}000 \times 10^{12}$ moles/K yr, Holland (1978) concludes that the present atmospheric O_2 level is at or close to steady state.

2.2. Coupling of Carbon–Oxygen Geochemical Cycles

Several important questions follow the overall model for atmospheric oxygen proposed by Holland. For example, "How stable is the present steady state p_{O_2} value?," "What may cause instability of the p_{O_2}?," "If a change in p_{O_2} occurs, how long will it take to reach a new steady state?," "Will a new steady state be the same as the present one?"

The ultimate response of the oxygen geochemical cycle to perturbations is determined by both the shape and the intersection of the two overall fluxes (production and consumption) in Fig. 2. The intersection of the two fluxes, shown by the crossed circle in Fig. 2, determines the steady state oxygen content of the atmosphere. Given enough time under the given conditions, the atmosphere would evolve so that the p_{O_2} would have the value corresponding to the intersection of the two fluxes. This steady state value is of great interest, therefore, and will be investigated at length later in this paper. The shape of the overall flux curves around the intersection point will determine the stability of the oxygen geochemical cycle. More precisely, the slope of each curve at the intersection point controls how fast the geochemical cycle of oxygen will achieve steady state. This response time is important because for very long response times the geochemical cycle is unlikely to maintain all other conditions essentially constant and therefore a steady state is unlikely to ever to be reached.

To understand the possible variations of the oxygen content in the atmosphere requires establishing the dominant fluxes and concomitant chemical–biological–physical mechanisms of not just the oxygen geochemical cycle but also the carbon, sulfur, and iron geochemical cycles. According to Holland (1978), the average contents of reducing compounds in the upper crustal rocks are 0.45 wt. % organic carbon, 0.3 wt. % sulfide sulfur, and 1.9 wt. % "FeO." During weathering, one kilogram of such a rock can consume up to 12 g of O_2 by C, 6 g of O_2 by S^{2-}, and 2 g of O_2 by "FeO." That is, 60% of the O_2 consumption by soils may be carried out by organic C, 30% by sulfide sulfur, and 10% by FeO. Recent data on sulfur and carbon contents of Precambrian shales (e.g., Watanabe et al., 1997) suggest that the average content of sulfide sulfur in the upper crustal rocks is between 0.1 and 0.2 wt. %, rather than 0.3 wt. %. Therefore, we can safely assume that the organic carbon in sedimentary rocks is the principal consumer of atmospheric O_2 during soil formation. In our initial model we will focus on the coupling of the oxygen and carbon geochemical cycles. Later modifications can include the couplings to the sulfur and iron systems.

Figure 3 sketches the dominant mechanisms and reservoirs important to the geochemical cycles of both carbon and oxygen. Table 1 gives values for some of the various reservoirs and fluxes. All reservoir sizes in this paper will be given in typical global units of 10^{12} moles. For the time scales of interest here, a convenient unit of time is 1000 years. The fluxes will then be given in units of 10^{12} moles/K yr. Present-day fluxes are indicated by the superscript "0."

Besides the oxygen reservoir, M_{O_2}, four reservoirs in Fig. 3 will be of significance in our quantification of atmospheric p_{O_2}. These reservoirs are the total content of carbonates in the crust, M_{carb}, the total organic C in the crust, M_{org}, the total CO_2 ($+ HCO_3^-$) in the atmosphere + ocean system, $M_{\Sigma CO_2}$, and the content of fossil organic carbon in soils, $M_{s,org}$. The kinetic equations for $M_{s,org}$ will be developed in the next section. Based on the reservoirs and fluxes in Fig. 3, the equations of motion for the oxygen and carbon reservoirs are

$$\frac{dM_{O_2}}{dt} = F_{b,org} - F_{v,redC} - F_{v,redH} - F_{w,org}, \quad (5)$$

$$\frac{dM_{org}}{dt} = F_{b,org} - F_{sub,org} - F_{w,org}, \quad (6)$$

$$\frac{dM_{carb}}{dt} = F_{b,carb} - F_{w,carb} - F_{sub,carb}, \quad (7)$$

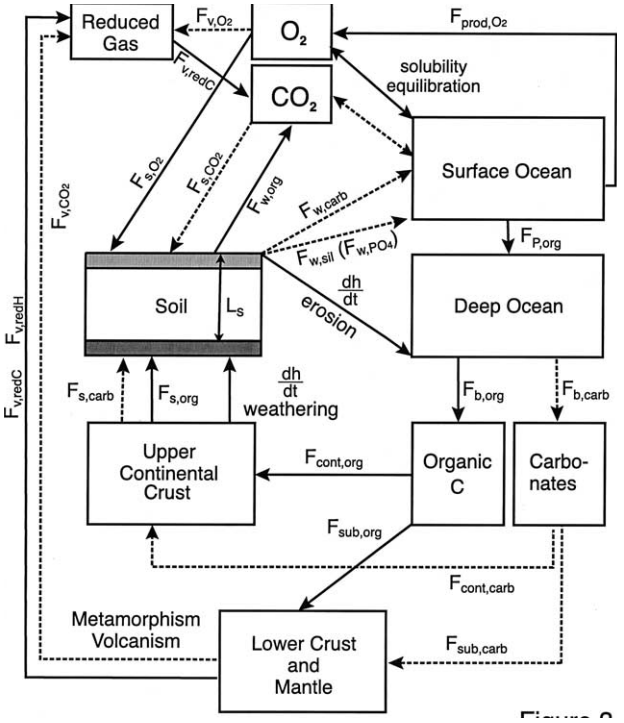

Fig. 3. The reservoirs and fluxes in our model. Abbreviations are b = burial, s = soil, p = phosphate, v = volcanic, w = weathering, carb = carbonate, cont = continent, org = organic C, redC = C-bearing reduced gases (CO, CH_4), redH = non-C-bearing reduced gases (H_2, H_2S, SO_2), sub = subduction, and dh/dt = physical erosion rate.

$$\frac{dM_{\Sigma CO_2}}{dt} = F_{v,CO_2} + F_{v,redC} + F_{w,carb} + F_{w,org} - F_{b,carb} - F_{b,org}. \tag{8}$$

F_{v,O_2} has been decomposed into C-bearing ($F_{v,redC}$) and non-C-bearing ($F_{v,redH}$) reduced gases (see below). The subscripts "sub" and "w" refer to "subduction" and "weathering," respectively. Equations (5)–(8) are the fundamental kinetic equations that determine the geochemical evolution and the dynamic behavior of the CO_2–O_2 coupled system.

The p_{CO_2} of the atmosphere is assumed to track the total amount of CO_2 in the ocean–atmosphere system, $M_{\Sigma CO_2}$. We assume that the oceans are always saturated with calcite and that they are in equilibrium with the atmospheric CO_2 through the following reaction:

$$Ca^{2+} + 2\,HCO_3^- \rightarrow CaCO_3 + CO_2 + H_2O. \tag{9}$$

If $M_{\Sigma CO_2}$ is associated with the amount of HCO_3^- in the oceans, then the last chemical reaction suggests

$$p_{CO_2} = K'\,M_{\Sigma CO_2}^2$$

assuming that m_{Ca} is greater than m_{HCO_3} and therefore relatively constant. (If the case arose that m_{Ca} was comparable to and covarying with m_{HCO_3}, then the proportionality would be closer to cubic rather than quadratic; however, we will ignore this here.) Therefore, just as done by Kump and Arthur (1999), the simple relation

$$p_{CO_2} = p_{CO_2}^0 \left(\frac{M_{\Sigma CO_2}}{M_{\Sigma CO_2}^0}\right)^2 \tag{10}$$

will be used.

To solve eqns. (5)–(8), it is essential to delineate the dependence of the various fluxes on any of the global properties in the coupled carbon–oxygen–geochemical cycle. The most important fluxes, $F_{b,org}$ and F_{s,O_2}, will be discussed at length in the next two sections. The present day value of $F_{b,org}$, based on Holland (1978), will be taken as

$$F_{b,org}^0 = 10{,}000 \times 10^{12}\ \text{moles/K yr}. \tag{11}$$

The carbonate burial flux, $F_{b,carb}$, is simply governed by the input of alkalinity into the oceans. Alkalinity is input from both silicate weathering and carbonate weathering. Although we do not treat the silicate rock reservoir explicitly in Fig. 3, we include the silicate weathering fluxes. Therefore,

$$F_{b,carb} = F_{w,sil} + F_{w,carb}. \tag{12}$$

According to Kump and Arthur (1999), $F_{w,sil}^0 = 6000$ and $F_{w,carb}^0 = 34{,}000$ in 10^{12} moles/K yr. The weathering of silicates depends on temperature and pH, which in turn are dependent on p_{CO_2} [Berner, Lasaga, and Garrels (BLAG, 1983); Lasaga et al., 1985; Brady 1991). The silicate weathering flux, $F_{w,sil}$, also depends on the total continental land area, A_{land}. Therefore,

$$F_{w,sil} = F_{w,sil}^0 \left(\frac{p_{CO_2}}{p_{CO_2}^0}\right)^{x_{CO_2,sil}} \frac{A_{land}}{A_{land}^0} \tag{13}$$

The value for the exponent, x_{CO_2}, can be obtained from curves such as in BLAG (1983), which yields

$$x_{CO_2,sil} \sim 0.25. \tag{14}$$

The term "land area," A_{land}, is used in our model as "the total land area for soil development." Therefore, its value depends on the global conditions for climate and geographical distributions of lands. For example, even when the true land area remains the same, A_{land} can become larger if the land masses are divided into smaller fragments and distributed in an equatorial region compared to a situation where all land mass occurs in a higher latitude region as one supercontinent.

By similar reasoning, the carbonate weathering flux is given by

$$F_{w,carb} = F_{w,carb}^0 \left(\frac{p_{CO_2}}{p_{CO_2}^0}\right)^{x_{CO_2,carb}} \frac{A_{land}}{A_{land}^0} \frac{M_{carb}}{M_{carb}^0} \tag{15}$$

with the additional dependence on the abundance of carbonates, M_{carb}. We will assume that

$$x_{CO_2,carb} = 0.5 \tag{16}$$

as done by other workers (e.g., Berner, 1991).

The volcanic flux of CO_2, F_{v,CO_2}, represents the sum total of decarbonation reactions (e.g., metamorphism and volcanism). Therefore, this flux will depend on the abundance of carbonates, M_{carb}, and on the intensity of plate tectonics, $I_{tectonics}$. As a result,

$$F_{v,CO_2} = F^0_{v,CO_2} \frac{M_{carb}}{M^0_{carb}} \frac{I_{tectonics}}{I^0_{tectonics}}, \quad (17)$$

where

$$F^0_{v,CO_2} = 6000 \times 10^{12} \text{ moles/K yr.}$$

When the production flux of O_2 is greater than the fluxes of reduced gases, essentially all the reduced gasses are quickly oxidized through photochemical reactions in the atmosphere. Therefore, we adopt the following simplified relation:

$$F_{v,O_2} = F_{v,red} \text{ if } F_{prod,O_2} \geq F_{v,red}. \quad (18)$$

Reduced gases from volcanism, metamorphism, and hydrothermal activities are divided into C-bearing reduced gases (primarily CO and CH_4) and noncarbon-bearing reduced gases (primarily H_2, H_2S, and SO_2). Thus,

$$F_{v,red} = F_{v,redC} + F_{v,redH}. \quad (19)$$

This treatment of reduced gases is made because the fluxes of carbon-bearing reduced gases directly affect the $M_{\Sigma CO_2}$ value, but the fluxes of the other reduced gases do not [see Eqn. (8)]. Using the ratio of present burial fluxes of organic carbon to carbonate carbon in sediments, 1/4, we assume that

$$F_{v,redC} = \frac{1}{4} F_{v,CO_2}. \quad (20)$$

Therefore, taking into consideration the values suggested by Holland (1978), we assume the following values for present-day fluxes:

$$F^0_{v,redC} = 1500 \times 10^{12} \text{ moles/K yr}, \quad (21)$$

$$F^0_{v,redH} = 1000 \times 10^{12} \text{ moles/K yr}. \quad (22)$$

Our model assumes that total carbon is conserved in the atmosphere–oceans–crust–mantle system. To ensure conservation of total carbon, the sum of Eqns. (6), (7), and (8) must add to zero. This condition requires that

$$F_{sub,carb} = F_{v,CO_2} \quad (23)$$

and

$$F_{sub,org} = F_{v,redC}. \quad (24)$$

3. O_2 OXIDATION FLUX INCLUDING SOIL DYNAMICS AND EROSION

The soil oxidation flux, F_{s,O_2}, can be quantified by including the chemical and physical behavior of soils explicitly (see Fig. 3). Introducing soils into the model highlights the importance of coupling both physical and chemical weathering in the oxygen (and carbon dioxide) geochemical cycles. We shall label $M_{s,org}$ the total amount of fossil organic matter in soils. As sedimentary rocks with organic matter are weathered, new material is input into the soil reservoir (Fig. 3). At the same time, physical erosion of soils leads to sediment yield carried by rivers and a flux from the soil reservoir to the oceans. In addition, chemical reactions take place in soils. The oxidation of fossil organic matter in soils will be treated explicitly using the recent kinetic data on oxidation of refractory (coal, kerogen graphite) organic matter (Chang and Berner, 1999). Note that, while silicate weathering is included in the treatment of CO_2 and alkalinity, the soil dynamics of silicate weathering will not be treated explicity (unlike our treatment of fossil organic matter) in this paper.

3.1. Mechanisms of Oxidation of Organic Matter

Chang and Berner (1999) measured a $p_{O_2}^{1/2}$ dependence for the oxidation rate of coal in an oxygenated aequous environment. The dependence of the rate on $p_{O_2}^{1/2}$ is expected if dissociation of the diatomic oxygen molecule takes place at the surface of the organic matter. Appendix A gives a probable mechanism for this dependence based on what we know from heterogeneous reaction kinetics. For the kinetics of oxidation of fossil organic matter in soils, therefore, we adopt the following rate law:

$$F_{s,O_2} = k_+ A_{s,org} p_{O_2}^{1/2}, \quad (25)$$

where k_+ is the heterogenous rate constant and $A_{s,org}$ is the total surface area of organic matter exposed to subaerial oxidation. The value of k_+ under aerated conditions ($p_{O_2} = 1$ PAL) in the presence of water at 25°C was determined to be

$$k_+ = 2 \times 10^{-12} \text{ moles C/m}^2\text{/s} = 0.063 \text{ moles C/m}^2\text{/K yr}. \quad (26)$$

The oxidation of organic carbon in soils is a heterogenous reaction and therefore depends on the surface area of fossil organic matter exposed to oxidation. The total surface area of organic matter in the global soil reservoir, $A_{s,org}$, is related to the specific surface area of organic matter in soils, $\bar{A}_{org}$, which depends on the size of individual organic matter particles; to the content of organic carbon in soil, $W_{s,org}$ (wt. %); to the total surface area of soil-forming lands, A_{land}; to the average depth of soils, L_s; to the density of soils, ρ_s, and to the mechanical erosion rate of soils, dh/dt. Note that in this entire treatment the organic matter involved is the refractory fossil organic matter. Highly decomposable organic matter, such as the remnant of soil-surface biomats and organisms in soils, is very quickly oxidized. This quick formation and destruction of organic matter cancels out in the long-term (even years) treatment of oxygen in the atmosphere and is not important to us here. Note also that the usual action by bacteria in oxidizing metabolizable organic matter refers to this decomposable organic matter and not to the highly refractory and bacterially undesirable fossil organic matter. Thus, it is very reasonable to expect that the laboratory kinetic data from Chang and Berner (1999) would be precisely applicable to the important oxidation flux, F_{s,O_2}, in the oxygen cycle. The results will be explored in the next few sections.

3.2. Derivation of the Rate Equations

To treat the oxidation of the refractory organic matter introduced from sedimentary rocks, we will assume that the organic matter comes in the shape of platelets with dimensions, 50 μm × 50 μm × 10 μm, a typical size of organic matter in shales (Watanabe, personal communication, 1999). One can calculate the specific surface area, $\bar{A}_{org}$, of such platelets if the

density of the organic matter is known. Using the density of graphite (2.26 g/cm^3), one obtains

$$V_{\text{platelet}} = 2.5 \times 10^{-8}\ \text{cm}^3,$$

$$A_{\text{platelet}} = 7 \times 10^{-5}\ \text{cm}^2,$$

$$1\ \text{g} = 0.44\ \text{cm}^3 = 1.76 \times 10^7\ \text{platelets} = 1.2 \times 10^3\ \text{cm}^2.$$

Therefore,

$$\bar{A}_{\text{org}} = 0.12\ \text{m}^2/\text{g}. \tag{27}$$

The uncertainty in the average dimensions of organic matter in sedimentary rocks may be as high as 50%. If the dimensions of the platelets are within a range of $(50 \pm 20) \times (50 \pm 20) \times (10 \pm 5)\ \mu$m, the range of $\bar{A}_{\text{org}}$ becomes between 0.08 and 0.23 m^2/g. Note that the study of Chang and Berner (1999) used a BET adsorption isotherm to estimate the surface area of their coal. We are substituting our calculation of the geometric surface area as the best estimate of the specific surface area of the fossil organic matter.

It is very useful to explore the implications of the fossil organic matter oxidation rate on the fate of our soils. Using the relation

$$\frac{dr}{dt} = k_+ \bar{V} \tag{28}$$

(Lasaga, 1998) between the rate of movement of the surface, dr/dt, and the reaction rate constant, k_+, where $\bar{V}$, is the molar volume, it can be concluded that for coal

$$\frac{dr}{dt} = (2 \times 10^{-12}\ \text{molesC/m}^2\text{/s})\ (5.3\ \text{cm}^3\text{/mole})\ (10^{-4}\ \text{m}^2/\text{cm}^2)$$

$$= 10^{-15}\ \text{cm/s}.$$

Based on our organic matter platelets, the oxidation half-life for a distance of 25 μ (half the distance from either end) would then be

$$\tau_{\text{oxidation}} = \frac{2.5 \times 10^{-3}\ \text{cm}}{10^{-15}\ \text{cm/s}} = 85{,}000\ \text{years}.$$

It is interesting that this length of time is comparable to the average residence time of soils (108,000 years, Lasaga et al., 1994). The comparable size of the two durations suggests some nontrivial dynamics in coupling physical erosion to chemical oxidation (and F_{s,O_2}), as will be shown below.

Normally chemical reactions lead to gradients in weathering with depth of the soils. In our treatment we will mix the soil so that chemical changes occur uniformly throughout the depth, L_s, of the soil (see Fig. 3). This depth, L_s, marks the area of high permeability which is most accessible to reaction. It is not clear what the average depth of soils, L_s, is today. L_s can clearly vary from very high values in the tropics to very low values in desert areas. It is expected that L_s may be somewhere between 1 m and 10 m. However, in prevascular plant earth conditions, the value of L_s was probably lower than today's value. In this paper, we will let L_s range from 1 m to 10 m to illustrate the possible importance of L_s on the overall dynamics of the system.

The soil will be assumed to have a uniform (but variable) organic content, labeled by $W_{s,\text{org}}$ in wt. %. For the source rock, we will assume an average content of organic matter, $W_{r,\text{org}}$. $W_{r,\text{org}}$ can be evaluated assuming that 75% of exposed rocks are sedimentary rocks and 25% are igneous and metamorphic rocks (Holland, 1978). Furthermore, the sedimentary rocks are assumed to consist of 60% shales (0.9 wt. % org C), 20% carbonates (0.2 wt. % org C) and 20% sandstones (0.05 wt. % org C) (Holland, 1978). The average organic content of rocks will then be taken as

$$W_{r,\text{org}} = [(0.9\%)(0.6) + (0.2\%)(0.2) + (0.05\%)(0.2)]\ 0.75,$$

$$W_{r,\text{org}} = 0.44\ \text{wt. \%}. \tag{29}$$

To incorporate the chemical oxidation kinetics into our global model, we will make the simplifying assumption that the organic matter specific surface area, $\bar{A}_{\text{org}}$, does not change during weathering. In reality, as the organic content drops due to oxidation, the platelet sizes will shrink and increase $\bar{A}_{\text{org}}$. For example, the change of sizes from $50 \times 50 \times 10\ \mu$m to $20 \times 20 \times 10\ \mu$m will increase the $\bar{A}_{\text{org}}$ value from 0.12 to 0.18 m^2/g. Such a change will be ignored for our first treatment. With this last assumption, we are ready to derive the equations relating F_{s,O_2} and the organic content in our soil reservoir, $W_{s,\text{org}}$, as a function of the relative changes in the other parameters.

The total surface area of organic matter in the global soil reservoir, $A_{s,\text{org}}$ (in units of m^2), can be related to the total mass of organic carbon in the soil reservoir, $M_{s,\text{org}}$ (in units of 10^{12} moles), and the specific surface area of organics by

$$A_{s,\text{org}} = 12 \times 10^{12}\ M_{s,\text{org}}\ \bar{A}_{\text{org}}\ \text{m}^2. \tag{30}$$

$M_{s,\text{org}}$ is related to the organic carbon content, $W_{s,\text{org}}$ (in units of wt. %), the total area of continents, A_{land} (in units of m^2), the average soil depth, L_s (in units of m), and the soil density, ρ_s (in units of g/cm^3) by

$$M_{s,\text{org}} = \frac{W_{s,\text{org}}}{100} A_{\text{land}}\ L_s\ 10^6\ \rho_s \frac{1}{12} \frac{1}{10^{12}},$$

$$M_{s,\text{org}} = 8.3 \times 10^{-10}\ W_{s,\text{org}}\ A_{\text{land}}\ L_s\ \rho_s\ 10^{12}\ \text{moles}. \tag{31}$$

Substituting Eqns. (26), (30), and (31) into the general rate law for the oxidation of organic matter (25), leads to our expression for the oxidation consumption of oxygen in our system:

$$F_{s,O_2} = k_+ A_{s,\text{org}} \left(\frac{p_{O_2}}{p^0_{O_2}}\right)^{1/2} \cdot\ 10^{-12}$$

$$= 0.063(12 \times 10^{12})\ \bar{A}_{\text{org}}\ (8.3 \times 10^{-10})$$

$$\cdot\ W_{s,\text{org}}\ A_{\text{land}}\ L_s\ \rho_s \left(\frac{p_{O_2}}{p^0_{O_2}}\right)^{1/2} \cdot\ 10^{-12}$$

or

$$F_{s,O_2} = (6.3 \times 10^{-10})\ \bar{A}_{\text{org}}\ W_{s,\text{org}}\ A_{\text{land}}\ L_s\ \rho_s \left(\frac{p_{O_2}}{p^0_{O_2}}\right)^{1/2}$$

$$\text{in } 10^{12}\ \text{moles/K yr}. \tag{32}$$

Inserting the expression for $M_{s,org}$ in Eqn. (32), we can rewrite this as

$$\text{Soil Oxidation Rate} = F_{s,O_2} = 0.72\,\bar{A}_{org}\,M_{s,org}\left(\frac{p_{O_2}}{p^0_{O_2}}\right)^{1/2}, \tag{33}$$

where $\bar{A}_{org}$ is in m^2/g, $M_{s,org}$ is in 10^{12} moles and F_{s,O_2} is in 10^{12} moles/K yr (the 0.72 factor assumes these units).

The formulation of F_{s,O_2} in Eqn. (32) or (33) is not based on the estimate of global oxidation rate today. Equation (33) is using actually measured kinetic data for refractory organic matter rather than fudging the global oxidation flux from a box model. We can, therefore, test the kinetic formulation by using present-day values for $W^0_{r,org}$ (0.44 wt. %), A^0_{land} (1.5×10^{14} m^2), L_s (5 m), and ρ_s (2.6 g/cm^3). In reality, the $W_{s,org}$ value decreases during soil formation from its value in the parent rock. If the remaining organic matter is 10% of the original, $W^0_{s,org} = 0.062$ wt. % (see also below). With these values, Eqns. (30), (31), and (33) yield

$$M^0_{s,org} = 1 \times 10^5 \times 10^{12} \text{ moles},$$

$$A^0_{s,org} = 0.725 \times 10^{18}\ m^2,$$

$$F_{s,O_2} = 0.72\ (0.12)\ (1 \times 10^5) = 8640 \times 10^{12} \text{ moles/K yr}.$$

Since the present-day production flux of O_2 is about $10{,}000 \times 10^{12}$ moles/K yr, the calculated value of F_{s,O_2} indicates that the oxidation flux by soil corresponds closely to the present-day value. It is quite important to emphasize that the measured kinetic data and a model that has an oxygen feedback in the oxidation of organic matter can predict quite nicely the behavior of the oxygen geochemical cycle today. This result is contrary to the usual assumption that the oxidation kinetics are not important and that only the erosion rate is important in determining the oxygen sink via oxidation reactions (e.g., Holland, 1978; Chang and Berner, 1999). We shall elaborate on this important point further below.

In addition to the chemical reaction taking place, new soil is being produced from rocks and current soil is physically eroded and dumped into the oceans (see Fig. 3). A very important parameter now enters the picture, the erosion rate, dh/dt. Based on erosion data from Holland (1978) among others, the physical erosion rate today is around 0.005 cm/yr. We will assume that the soil system per se is in steady state so that the average depth L_s (Fig. 3) does not vary. In what follows, both parameters, dh/dt and L_s, will be separately varied. This variation is not meant to imply that dh/dt and L_s are not coupled. On the contrary, it is almost certain that the value of dh/dt and the topography of the land area (especifically the slope of the weathering zones) will determine the value of L_s. However, in this initial treatment of coupled physical and chemical erosion, we do not carry out this coupling explicitly. In part, this coupling would require a much more detailed model of the land topography than included in our current model. In addition, the variations of dh/dt and L_s reflect also our ignorance of what are the appropiate global L_s values not only in the past, but even today. We hope that future studies will, in fact, take this problem to much higher levels of development.

A given erosion rate, dh/dt in cm/yr, will remove dh/dt cm from the soil in one year and also add dh/dt cm of new soil in that year from the rocks beneath. If $W_{r,org}$ is the wt.% organic content of the rock, then the new amount of organic matter added to the soil is given by

$$+\left.\frac{dM_{s,org}}{dt}\right|_{\text{new soil}} = 10^7\,\frac{dh}{dt}\,A_{land}\,\alpha_{conv}\,\rho_{rock}\,\frac{W_{r,org}}{100}\,\frac{1}{12}\,\frac{1}{10^{12}} \times 10^{12} \text{ moles/K yr}. \tag{34}$$

The parameter α_{conv} takes into account that usually it takes more than 1 g of rock to make 1 g of soil (due to losses); therefore, α_{conv} is always greater than 1. In our calculations, we have chosen a typical value of α_{conv} as 1.4 (e.g., Carroll, 1970; Drever, 1997).

The removal of soil due to physical weathering will lead to a loss of organic carbon:

$$-\left.\frac{dM_{s,org}}{dt}\right|_{\text{Erosion Loss}} = 10^7\,\frac{dh}{dt}\,A_{land}\,\rho_{soil}\,\frac{W_{s,org}}{100}\,\frac{1}{12}\,\frac{1}{10^{12}} \times 10^{12} \text{ moles/K yr}. \tag{35}$$

Again, using our expression for $M_{s,org}$ [Eq. (3)], the loss can be rewritten as

$$-\left.\frac{dM_{s,org}}{dt}\right|_{\text{Erosion Loss}} = 10\frac{dh}{dt}\,\frac{M_{s,org}}{L_s}. \tag{36}$$

In addition to the input of organic matter from new soil formation and the loss of organic matter from soils by physical erosion, organic matter will be lost by the same oxidation rate calculated earlier, F_{s,O_2}. Altogether, then, the overall equation for the changes in the organic matter in soils (and indirectly the oxidation rate) is given by

$$\frac{dM_{s,org}}{dt} = 10\,\frac{dh}{dt}\left(8.3 \times 10^{-10} A_{land}\,\alpha_{conv}\,\rho_{rock}\,W_{r,org} - \frac{M_{s,org}}{L_s}\right) - 0.72\bar{A}_{org}\,M_{s,org}\left(\frac{p_{O_2}}{p^0_{O_2}}\right)^{1/2}. \tag{37}$$

Equation (37) is the key equation that brings in both chemical and physical weathering into the overall treatment of the oxygen geochemical cycle. Note that some of the new key parameters are the soil depth, L_s, the specific surface area of organic matter, $\bar{A}_{org}$, and the erosion rate, dh/dt. In addition, $W_{r,org}$ in Eqn. (37) will change in a manner proportional to changes in M_{org}, that is

$$W_{r,org} = W^0_{r,org}\left(\frac{M_{org}}{M^0_{org}}\right). \tag{38}$$

3.3 $W_{s,org}$ and F_{s,O_2} at Steady State

The soil quantities, $M_{s,org}$ and $W_{s,org}$ will, under many circumstances, reach steady state ($dM_{s,org}/dt = 0$). We can use Eqn. (37) to solve for $M_{s,org}$ at steady state:

$$M_{s,org} = \frac{8.3 \times 10^{-9}\frac{dh}{dt}\,A_{land}\,\alpha_{conv}\,\rho_{rock}\,W_{r,org}}{\frac{10}{L_s}\frac{dh}{dt} + 0.72\,\bar{A}_{org}\left(\frac{p_{O_2}}{p^0_{O_2}}\right)^{1/2}}. \tag{39}$$

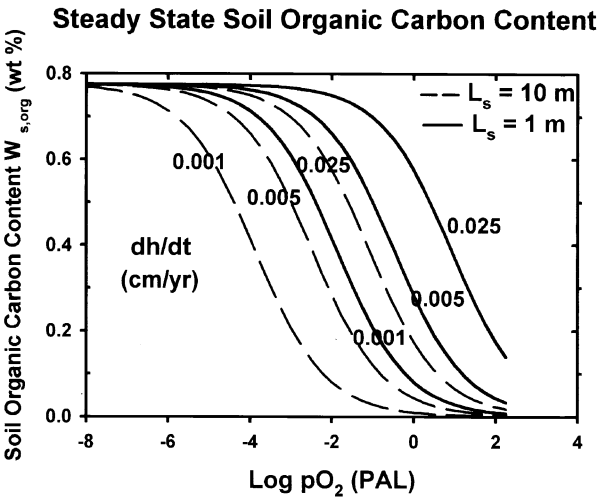

Fig. 4. The steady-state soil organic carbon content, $W_{s,\mathrm{org}}$ (wt. %), as a function of the atmospheric p_{O_2} and the physical erosion rate (dh/dt). Solid lines corresponds to soil depths $L_s = 1$ m and dashed lines to $L_s = 10$ m. The organic C content of the fresh rock, $W_{r,\mathrm{org}} = 0.44$ wt. % and $\alpha_{\mathrm{conv}} = 1.4$.

Likewise from Eqn. (31), the steady state value of $W_{s,\mathrm{org}}$ is given by

$$W_{s,\mathrm{org}} = \frac{\dfrac{10}{L_s}\dfrac{dh}{dt}\,\alpha_{\mathrm{conv}}\,\dfrac{\rho_{\mathrm{rock}}}{\rho_s}\,W_{r,\mathrm{org}}}{\dfrac{10}{L_s}\dfrac{dh}{dt} + 0.72\bar{A}_{\mathrm{org}}\left(\dfrac{p_{O_2}}{p^0_{O_2}}\right)^{1/2}}. \tag{40}$$

For example, if $dh/dt = 0.005$ cm/yr, $W_{\mathrm{r,org}} = 0.44$ wt. %, $\alpha_{\mathrm{conv}} = 1.4$, $\bar{A}_{\mathrm{org}} = 0.12$ m^2/g, $L_s = 1$ m, $p_{O_2} = 0.2$ bar, $\rho_r = 2.5$ g/cm^3, and $\rho_s = 2.0$ g/cm^3, then the steady state value of soil organic content, $W_{s,\mathrm{org}} = 0.284$ wt. %. This indicates that more than half the organic matter in soils is decomposed during chemical weathering, and the remaining steady state content is physically transported as a detrital mineral.

Using Eqn. (40), the steady state organic carbon content of soil is computed as a function of soil depth, erosion rate and p_{O_2} in Fig. 4. Figure 4 indicates that at $p_{O_2} < 10^{-3}$ PAL, only a very small fraction of soil organic matter is decomposed by oxidation. In this case, the average organic carbon content of soils is that of the parental rocks except for the α_{conv} and density correction [i.e., $W_{s,\mathrm{org}} = 0.44$ wt. % (1.4)(2.5/2.0) = 0.775 wt. %] and essentially all the soil organic carbon is recycled back to the oceans as a detrital mineral.

Equation (39) can be used to write the oxidation flux in terms of just O_2, i.e., using Eqn. (33):

$$F_{s,O_2} = \frac{0.72\,\bar{A}_{\mathrm{org}}\,F_{\mathrm{limit}}\left(\dfrac{p_{O_2}}{p^0_{O_2}}\right)^{1/2}}{\dfrac{10}{L_s}\dfrac{dh}{dt} + 0.72\bar{A}_{\mathrm{org}}\left(\dfrac{p_{O_2}}{p^0_{O_2}}\right)^{1/2}}, \tag{41}$$

where the limit flux in the numerator is given by

$$F_{\mathrm{limit}} \equiv 8.3 \times 10^{-9}\,\frac{dh}{dt}\,A_{\mathrm{land}}\,\alpha_{\mathrm{conv}}\,\rho_{\mathrm{rock}}\,W_{\mathrm{r,org}}. \tag{42}$$

Equation (41), one of the key equations derived from this study, relates the steady state oxidation flux by weathering to the physical erosion rate, the specific surface area of organic matter, the organic carbon content of the parental rocks, the density of soils, the average depth of soils, the continental land area, and the atmospheric p_{O_2}.

Equation (41) can be used to explore a number of important dynamical questions in the oxygen geochemical cycle. A fundamental conclusion from Eqn. (41) is that, as the oxygen levels reach very high amounts, there is a finite upper bound for the oxidation flux, i.e., $F_{s,O_2} \to F_{\mathrm{limit}}$ as $p_{O_2} \to \infty$. F_{limit} is the limiting oxidation flux and it depends on the erosion rate and the exposed continental land area among other variables [see Eqn. (42)]. The limit arises because the oxidation flux cannot exceed the oxidation of the entire rock assemblage being weathered each year. Note that because of the soil dynamics, the net dependence of the oxidation rate on O_2 is more complicated than a square root dependence. In fact, in a manner akin to the Michaelis–Menten kinetics of biologists, the oxygen dependence of the oxidation rate ranges from a square root one to no dependence at all. Nonetheless, F_{s,O_2}, does increase monotonically with increasing O_2, thereby providing a negative feedback. The problem is that the negative feedback has diminishing power at very high O_2 levels.

Figure 5 clearly shows the increasing leveling of the F_{s,O_2} curve as dh/dt goes to very low values. Note the logarithmic scale for F_{s,O_2}. The figure indicates that, at $p_{O_2} < 10^{-3}$ PAL, the logarithm value of F_{s,O_2} increases linearly with increasing $\log(p_{O_2})$ with a slope of 0.5 but it is independent of the erosion rate. At p_{O_2} values between 10^{-3} and 10^2 PAL, F_{s,O_2} increases with increasing p_{O_2} and increasing erosion rate. For p_{O_2} greater than 10^2 PAL, F_{s,O_2} is independent of p_{O_2}. Such characteristics of F_{s,O_2} can be explained by examining the relative magnitude of the two terms in the denominator of Eqn. (41).

It is important to relate the kinetic Eqn. (41) for F_{s,O_2} to the common assumption that only rock exposure affects the oxidation rate of rocks. Most earlier statements on the geochemical cycle of oxygen have not considered the kinetics quantitatively as even our simple model has done. It is clear that the overall chemical kinetics are fast on a time scale of 1 million years. Nonetheless, given the dynamics of soil erosion, the chemical kinetics of oxidation are not independent of oxygen content. Quantitatively, what earlier workers have qualitatively alluded to is shown by taking the limit

$$\frac{dh}{dt} \to 0$$

in Eqn. (41). If the erosion rate were nearly zero, then indeed the oxidation flux would simply be F_{limit}, which is proportional to dh/dt and independent of p_{O_2}, as others have said. However, as Fig. 5 shows, current erosion rates are far removed from such low numbers.

Figure 5 shows that even in the case of an erosion rate 5 times lower than today (i.e., 0.001 cm/yr), the flux F_{s,O_2} may still be varying at todays values and has not reached the limiting value, F_{limit}. For the erosion rate to be such that oxygen levels make little difference on the oxidation flux would require

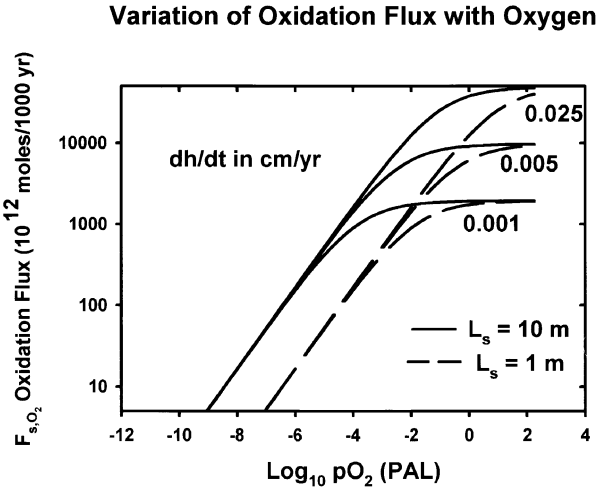

Fig. 5. Relationships between the O_2 consumption flux by soils, F_{s,O_2}, and the atmospheric p_{O_2} for different values of the erosion rate, dh/dt and of soil depth, L_s. F_{s,O_2} values are shown in log scale.

$$\frac{10}{L_s}\frac{dh}{dt} < 0.01 \cdot 0.72\, A_{\text{org}}.$$

For our given value of A_{org},

$$\frac{dh}{dt} < 0.0008 \text{ cm/yr } (L_s = 10 \text{ m})$$

or

$$\frac{dh}{dt} < 0.00008 \text{ cm/yr } (L_s = 1 \text{ m}).$$

3.4. The Steady State Oxygen Equation in the C–O Uncoupled System

In addition to deriving the function, F_{s,O_2}, the treatment above can be extended to obtain the steady state content of O_2 in the atmosphere. To do this, we will disregard all the important couplings to other subcycles such as the carbon cycle, which have been discussed in the earlier sections. If the net production flux of O_2 is given by F_{netprod,O_2}, then at steady state [see Eqn. (5)]:

$$F_{s,O_2} = F_{\text{net prod},O_2} = F_{b,\text{org}} - (F_{v,\text{redH}} + F_{v,\text{redC}}).$$

At first, we will treat $F_{b,\text{org}}$ as constant. Later, the oxygen feedback on $F_{b,\text{org}}$ will be added. For a given value of $F_{\text{net prod},O_2}$, Eqn. (41) for F_{s,O_2} can therefore be used in the previous equation to solve for the oxygen content of the atmosphere at steady state:

$$p_{O_2} \equiv p^0_{O_2} \frac{\left(\frac{10}{L_s}\frac{dh}{dt} F_{\text{net prod},O_2}\right)^2}{(0.72\, \bar{A}_{\text{org}})^2\, (F_{\text{limit}} - F_{\text{net prod},O_2})^2}. \qquad (43)$$

Figure 6 exhibits this dependence of oxygen levels on the various parameters on the right of Eqn. (43). Figure 6(A) shows the important dependence of p_{O_2} on the net production flux, $F_{\text{net prod},O_2}$, above. In Fig. 6(A) the erosion rate is held constant

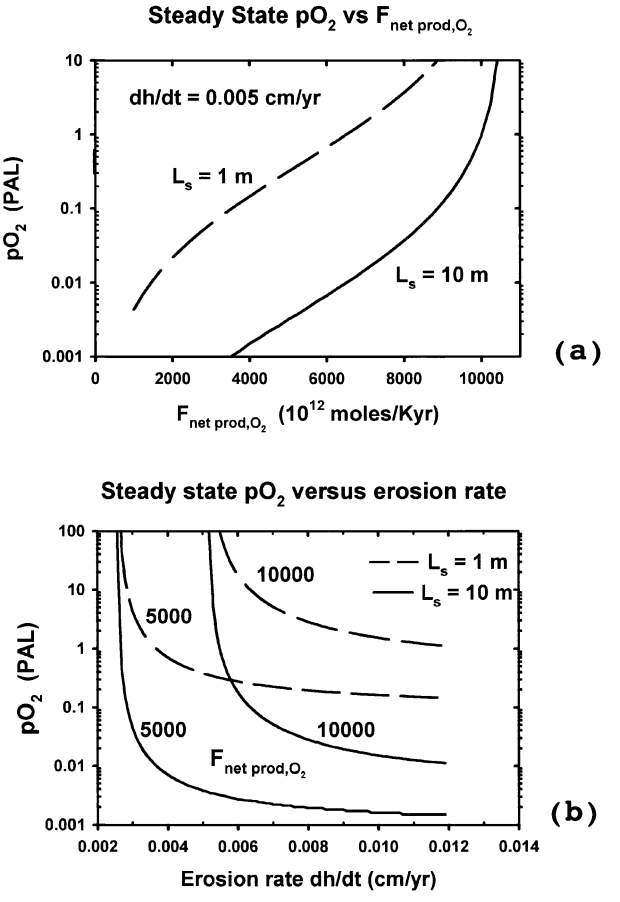

Fig. 6. The steady-state p_{O_2} values in the C–O uncoupled system. (a) Variation of p_{O_2} as a function of the net production flux, F_{netprod,O_2}. dh/dt is today's value and L_s = 1 m and 10 m. (b) Variation of p_{O_2} as a function of the erosion rate, dh/dt. Results are shown for both L = 1 m and 10 m and for $F_{\text{netprod},O_2} = 5000 \times 10^{12}$ moles/K yr and $10{,}000 \times 10^{12}$ moles/K yr.

close to today's value. Figure 6(B) illustrates the strong dependence of p_{O_2} on the erosion rate. These results should be contrasted with those given in the next section, which includes a strong feedback of oxygen on the burial flux, $F_{b,\text{org}}$. Equation (43) is rather interesting. It shows a quadratic dependence of the oxygen level on the erosion rate and on the burial flux. However, the denominator is very significant. Even if the net production flux is very small, if the limiting flux is also small (e.g., low organic carbon content of the rocks because $F_{\text{net prod},O_2}$ is small), then the denominator can offset decreases in the numerator and lead to high oxygen levels. The interplay between dh/dt, $F_{\text{net prod},O_2}$ and F_{limit} can be quite nontrivial.

3.5. Oxidation Flux and O_2 Response Time in the C–O Uncoupled System

If the oxidation of soils is an appropiate negative feedback in the oxygen cycle, contrary to the usual assumptions, then it would be useful to calculate an appropiate response time for the system based on only this negative feedback. To contrast this response time, it should be noted that today's oxygen cycle has a residence time given by

$$\tau_{residence} = \frac{M_{O_2}}{F_{\text{prod},O_2}} = \frac{38 \times 10^6}{10{,}000}\ 1000\ \text{yr} = 3.8\ \text{M yr}. \tag{44}$$

A response time can be evaluated by returning to the oxygen dynamic equation rewritten as

$$\frac{dM_{O_2}}{dt} = F_{\text{net prod},O_2} - F_{s,O_2}, \tag{45}$$

where

$$F_{\text{net prod},O_2} \equiv F_{b,\text{org}} - F_{v,\text{redH}} - F_{v,\text{redC}}. \tag{46}$$

The function F_{s,O_2} can then be expanded in a Taylor series:

$$F_{s,O_2} = F^{\text{ref}}_{s,O_2} + \frac{dF_{s,O_2}}{dM_{O_2\,\text{ref}}}(M_{O_2} - M^{\text{ref}}_{O_2}), \tag{47}$$

where $M^{\text{ref}}_{O_2}$ is the total amount of oxygen in the atmosphere and oceans at some appropriate reference value, F^{ref}_{s,O_2} is the value of F_{s,O_2} at this oxygen content, and $dF_{s,O_2}/dM_{O_{2\text{ref}}}$ is also evaluated at the particular reference oxygen content. Inputing Eqn. (47) into Eqn. (45) leads to

$$\frac{dM_{O_2}}{dt} = F_{\text{net prod},O_2} - F^{\text{ref}}_{s,O_2} - \frac{dF_{s,O_2}}{dM_{O_2\,\text{ref}}}(M_{O_2} - M^{ref}_{O_2}). \tag{48}$$

This equation has the form

$$\frac{dC}{dt} = a - kC,$$

where k is $dF_{s,O_2}/dMO_{2\text{ref}}$. Therefore, the response time of the system, in general, would be given by

$$\tau_{response} = \frac{1}{dF_{s,O_2}/dM_{O_2}}. \tag{49}$$

Carrying out the derivative of F_{s,O_2} in Eqn. (41) yields.

$$M_{O_2}\frac{dF_{s,O_2}}{dM_{O_2}} = \frac{0.36\,\bar{A}_{\text{org}}\,F'_{\text{limit}}\,\dfrac{dh}{dt}\left(\dfrac{p_{O_2}}{p^0_{O_2}}\right)^{1/2}}{\dfrac{10dh}{L_s\,dt} + 0.72\,\bar{A}_{\text{org}}\left(\dfrac{p_{O_2}}{p^0_{O_2}}\right)^{1/2}} - \frac{0.2592\,\bar{A}^2_{\text{org}}\,F'_{\text{limit}}\,\dfrac{dh}{dt}\left(\dfrac{p_{O_2}}{p^0_{O_2}}\right)}{\left[\dfrac{10}{L_s}\dfrac{dh}{dt} + 0.72\,\bar{A}_{\text{org}}\left(\dfrac{p_{O_2}}{p^0_{O_2}}\right)^{1/2}\right]^2} \tag{50}$$

in units of 10^{12} moles/K yr. F'_{limit} is the same as F_{limit} except that the dh/dt term was factored out:

$$F'_{\text{limit}} \equiv 8.3 \times 10^{-9} A_{\text{land}}\,\alpha_{\text{conv}}\,\rho_{\text{rock}}\,W_{r,\text{org}}. \tag{51}$$

Equations (49) and (50) can be used to calculate the response time for a variety of conditions. If we use the values of A_{org} (0.12 m^2/g), L (1 m or 10 m) and dh/dt (0.005 cm/yr) used earlier, the variation of the response time with the oxygen content is given in Fig. 7(A). The p_{O_2} value in the figure can be thought of as the steady state p_{O_2} value, which in turn, is

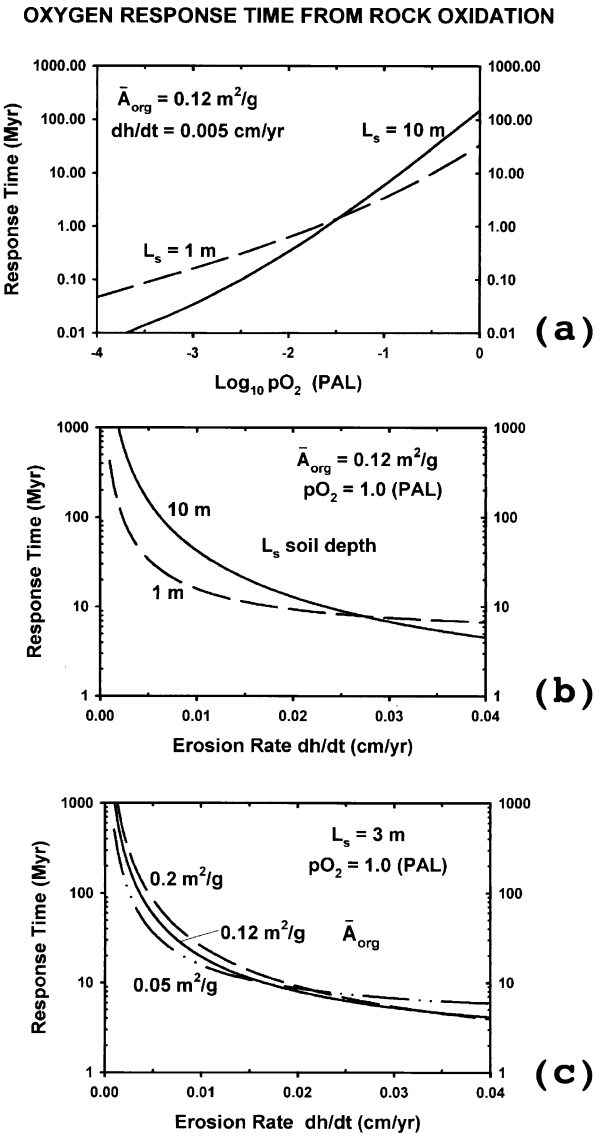

Fig. 7. The time to attain steady-state p_{O_2} values in the C–O uncoupled system. (a) Dependence on the oxygen content of the atmosphere for two different soil depths (L_s = 1 m and 10 m). (b) Dependence on the erosion rate, dh/dt, for oxygen contents equal to today's value and two different soil depths (L_s = 1 m and 10 m). (c) Dependence on the erosion rate, dh/dt, for different values of the organic specific surface area, $\bar{A}_{\text{org}}$ (in m^2/g).

determined by a value for the net production flux (e.g., as we increase the input of reduced gases, the steady state p_{O_2} can be dropped to 0.1 or 0.01 of today's value in this simple model). Note that for low p_{O_2}, the response time becomes extremely fast. For example, at p_{O_2} = 0.001 PAL, the response time is about 0.1 Ma. Even for a value of p_{O_2} equal to today's atmosphere, the response time is around 20–100 million years. While this value is certainly larger than the 4 million year "residence time", the response time is also far from infinity. Even for today's conditions, the soil oxidation negative feedback is a nontrivial stabilization of the oxygen cycle [e.g., Figs. 7(B) and (C)]. (It will be shown in a later section that, if the negative feedback by burial of organic carbon is included in the

model, the response time will become less than 2 Ma at p_{O_2} = 1 PAL.)

It is of interest, in fact, to keep the oxygen levels near today's values and study the effectiveness of the soil oxidation negative feedback as a function of the erosion dynamic variables: dh/dt, $\bar{A}_{org}$, and L_s. The variation of the response time with these variables is also shown in Figs. 7(B) and 7(C). Note the strong variation with dh/dt, as expected. A remarkable result is that for dh/dt values around 0.005 cm/yr, decreasing the depth of the soils, L_s, results in *faster* response times, contrary to what one would expect. This reversal is corrected only at high dh/dt's.

Increasing the specific surface area, $\bar{A}_{org}$, which is achieved by smaller grain sizes, would supposedly lead to faster kinetics and hence smaller response times. However, Fig. 7(C) illustrates that the reverse situation is valid for dh/dt values in the neighborhood of 0.005 cm/yr. Again, only higher dh/dt values make the curves cross and lead to the expected variation of the response time with A_{org}. In general, however, Fig. 7 shows that the soil oxidation negative feedback is much more effective than prior workers have assumed.

4. BURIAL FLUX OF ORGANIC MATTER

4.1. Theoretical Approach

The burial flux of new organic carbon, $F_{b,org}$, is related to the production flux of organic matter in the oceans, $F_{prod,org}$, by

$$F_{b,org} = \xi F_{prod,org}, \tag{52}$$

where ξ is the burial efficiency. The average ξ value in the present ocean is 0.003 (Holland, 1978), indicating that only 0.3% of the organic matter produced in the surface layer of the oceans escapes decomposition by aerobic and anaerobic organisms during settling on the seafloor and during the early diagenesis of sediments. The burial efficiency depends on the O_2 content of ocean water, and thus on the atmospheric p_{O_2}, Holland (1978) writes "If the oxygen content of the atmosphere and the oxygen content of surface water were reduced by a factor of 10, then not enough O_2 would be present in seawater to oxidize more than a small fraction of the organic matter produced photosynthetically in the upper parts of the oceans. Much of the ocean would, therefore, become anoxic, and a much larger quantity of organic matter would be buried, provided the present rate of photosynthesis could be maintained. Conversely, an increase in atmospheric O_2 would produce an increase in the O_2 content of seawater and hence a decrease in the burial rate of organic matter". Holland estimates that, under the same fluxes of nutrients (phosphates and nitrates) in the oceans, the maximum increase in the burial flux of organic matter is about 2 to 4 times of the present burial flux.

The organic burial term ultimately involves a combination of organic matter productivity in the surface oceans (the euphotic zone) and survival of the organic matter during settling in the ocean to be buried in sediments. The most illuminating handle on this problem comes from consideration of limiting nutrients, as has been done by many workers (Holland, 1978; 1984; Kump, 1988; Van Cappellen and Ingall, 1996; Lenton and Watson, 2000). In particular, the phosphate needed in DNA, RNA, and the energy ATP molecules seems to be the most likely candidate for limiting nutrient. (The nitrogen needed for all the amino acids in proteins seems to be less limiting, although a similar treatment could be developed along these lines. In this case, the phosphate input and output of the oceans will be very important fluxes. If the dominant removal of phosphate from the oceans is via sedimentation and if steady state is assumed for phosphate in the oceans, then

$$F_{w,P} = F_{b,P}, \tag{53}$$

where $F_{w,P}$ stands for the weathering flux of phosphate to the oceans and $F_{b,P}$ is the burial flux of phosphate into sediments. Note that the steady state assumption is not rigorously required. A serious imbalance could probably exist for 1 to 10 million years. But over 100 million years, any serious inbalance between inputs and outputs would lead to too great a change in the phosphorus content of the oceans. [The residence time is around 200,000 years for present-day conditions (Holland, 1978)]. Because the burial flux is an output, eventually the entire driving force for large fluctuations in the phosphate burial flux must come from changes in the weathering flux of phosphorus. Thus the weathering flux can triple leading to a tripling of the burial flux. But the burial flux cannot directly drive the weathering flux.

The total burial flux of phosphate, $F_{b,P}$, consists of the burial of P in organic matter and the burial of P in apatite, iron oxides or carbonates. The latter number seems to be about 20% of the river flux of phosphate (Holland, 1984). Let us call the nonorganic fraction of the burial flux of phosphate, γ. Then, the burial flux of organic phosphate is:

$$F_{b,org-P} = (1 - \gamma) F_{w,P}. \tag{54}$$

This organic P burial can be translated into the organic carbon burial of interest, $F_{b,org}$, if we know the molar C/P ratio, β, of the buried organic matter:

$$\beta \equiv \left(\frac{C}{P}\right)_{org}. \tag{55}$$

Note that in today's sediments, the C/P ratio is several times higher than the Redfield ratio, 106 (Holland, 1984). Altogether then

$$F_{b,org} = \beta (1 - \gamma) F_{w,P}. \tag{56}$$

Equation (56) can be used to derive the functional dependencies of $F_{b,org}$ on global parameters. First, the very important weathering flux of phosphate, $F_{w,P}$, depends on the weathering intensity for the breakdown of phosphate-containing shales, phosphorites, and apatites in igneous/metamorphic rocks. The variation in this weathering rate is similar to the variations discussed earlier and linked to changes in the continental land area and to CO_2 variations (e.g., temperature). Therefore, $F_{b,org}$ is varied according to

$$F_{b,org} = F^0_{b,org} \left(\frac{p_{CO_2}}{p^0_{CO_2}}\right)^{x_{CO_2,org}} \frac{A_{land}}{A^0_{land}} \tag{57}$$

where typically the exponent $x_{CO_2,org}$ was taken as equal to the silicate weathering exponent, $x_{CO_2,sil}$ in Eqn. (13). Because phosphate is not directly involved in oxidation/reduction processes, the weathering intensity has not been linked to p_{O_2}. The availability of phosphate for organisms in the oceans also

depends on the relative proportion of phosphate sinks (i.e., ferric hydroxides, organic matter, apatite) in the oceans, which may depend on the atmospheric p_{O_2} level (Van Cappellen and Ingall, 1996) and on the ocean circulation. However, in this paper we assume that the proportions of the various phosphate sinks and the ocean circulation will remain the same as today's values through the perturbations of other parameters.

The other term, β, does depend on the oxygen level of the atmosphere. β can be related to the fraction of organic matter that first survives oxidation during both settling in the oceans and burial in the anoxic part of sediments and second survives the subsequent sulfate reduction in early diagenesis. The C/P ratio of the buried organic matter depends on the relative destruction of the C-containing versus the P-containing organic functional groups.

Phosphate in organic matter exists in a variety of forms. Breaking down these groups is relatively easy. On the other hand, release of the C in organic matter requires breaking down and oxidizing the carbon in more stable organic molecules. This oxidation will depend on the oxygen content of deep ocean water, if the oceans are not anoxic. If the oceans are anoxic, then the breakdown will depend largely on oxidation of organic carbon by sulfate reducing bacteria.

Given the above considerations, the C/P β term was modeled by focusing on the destruction of the organic carbon by oxidation. The kinetics of oxygen-based bacterial oxidation of organic carbon was modeled in a manner similar to the sulfate-based bacterial oxidation kinetics in the pore waters of sediments (e.g., Berner, 1980; Lasaga, 1998). In particular, the kinetic oxidation rate law for marine organic matter was assumed to depend on the amount of organic matter, C, and on the oxygen content of the deep ocean via:

$$\text{Oxidation Rate} = \frac{dC}{dt} = -k\,C\,f, \tag{58}$$

where the function f has a Michaelis–Menten form

$$f = \frac{[O_2]_d}{K_{O_2} + [O_2]_d}. \tag{59}$$

$[O_2]_d$ is the deep ocean concentration of dissolved oxygen (in μM) and K_{O_2} is a Michaelis–Menten parameter. The same functionality, f, has been observed for the dependence of the kinetics of sulfate reduction on the sulfate content of the water (e.g., Boudreau and Westrich, 1984). One can integrate Eqn. (58) to obtain

$$C = C_0 e^{-k f t_{burial}}, \tag{60}$$

where t_{burial} refers to an average burial time for organic matter, i.e., the time during which the organic matter is susceptible to oxidation. We can use today's value for the fraction of the organic matter buried, 0.3%, to derive

$$\frac{C}{C_{0\ today}} = \frac{F^0_{b,org}}{F^0_{prod,org}} = \xi_{today} = 0.003 = e^{-k f_{today} t_{burial}}. \tag{61}$$

If we solve this equation for $k\,t_{burial}$:

$$k\,t_{burial} = \frac{-\ln(0.003)}{f_{today}}$$

and plug this value of $k\,t_{burial}$ into Eqn. (60), we obtain

$$\frac{F_{b,org}}{F_{prod,org}} \equiv \xi = (0.003)^{f/f_{today}}. \tag{62}$$

To obtain f, we need a value for $[O_2]_d$. The relation between p_{O_2} and $[O_2]_d$ can be derived using a simple three-box model of the oceans, with a low-latitude surface ocean, a high-latitude surface ocean and a deep ocean (Sarmiento and Toggweiler, 1984; Sarmiento, 1992). By assuming steady state for the phosphate and the oxygen concentrations in each of the three boxes, Sarmiento (1992) derives that

$$[O_2]_d = [O_2]_h - r_{O_2P}\,([PO_4^{3-}]_d - [PO_4^{3-}]_h), \tag{63}$$

where the subscripts d and h refer to the deep ocean and the high latitude surface ocean, respectively, and $[PO_4]$ stands for the concentration of phosphate in the respective box. r_{O_2} p is the ratio of moles of O_2 consumed per mole of organic P destroyed (i.e., the C/P ratio of the organic remains falling to the deep ocean). Using today's values for $r_{O_2/P}$, $[PO_4]_d$ and $[PO_4]_h$, we can rewrite this as

$$[O_2]_d = 340\frac{p_{O_2}}{p^0_{O_2}} - 172\ (2.2 - 1.2)\ \mu\text{M}. \tag{64}$$

One of the important conclusions from these simple models is the prediction of ocean anoxia even when p_{O_2} is not zero. In fact, Eqn. (64) predicts that

$$[O_2]_d = 0 \quad \text{when } p_{O_2} = 0.51\ p^0_{O_2}. \tag{65}$$

The inclusion of this link between p_{O_2} and $[O_2]_d$ in our model leads to a very nontrivial stabilization of the oxygen cycle. As p_{O_2} levels drop, the decrease in $[O_2]_d$ is even more severe based on Eqn. (64) and thus leads to a strong negative feedback via the reduced oxidation rates.

Once the oxygen levels drop significantly, *Desulfovibrio* bacteria can thrive and the organic matter will be destroyed by sulfate reduction in the water column, similarly to the processes going on today in the Black Sea. Based on Black Sea data (Arthur et al., 1994; Arthur and Dean, 1998), the fraction of organic matter that would survive just from sulfate reducers is 0.021, i.e., 7 times higher than the fraction today (see Fig. 8).

Altogether, then, we can postulate that the fraction buried, ξ (and by inference β and $F_{b,org}$) will vary according to

$$\xi = (0.003)^{f/f_{today}} \quad [O_2]_d > d_{min} \tag{66}$$

and

$$\xi = 0.021 \quad [O_2]_d \le d_{min}, \tag{67}$$

where d_{min} is a threshold oxygen concentration above which sulfate reducers cannot survive, f is given by Eqn. (59) and $[O_2]_d$ depends on p_{O_2} via Eqn. (64). Figure 9 illustrates the overall dependence of ξ on p_{O_2} in a case where $K_{O_2} = 20\ \mu$M and $d_{min} = 15\ \mu$M. Note the strong dependence on p_{O_2} as p_{O_2} drops significantly from 1 PAL and the much weaker dependence for high values of p_{O_2}.

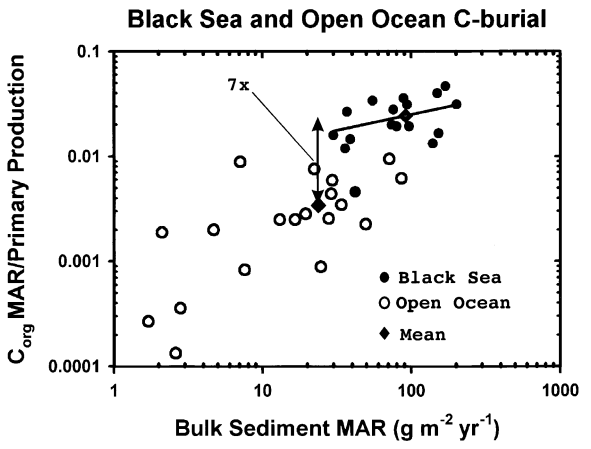

Fig. 8. Comparison of the burial efficiency, ξ, between the Black Sea and the open ocean (data from Arthur and Dean, 1998). The line through the Black Sea data has a slope of 0.30. The mean ξ values for the open ocean and the Black Sea data are shown by respective diamonds. MAR = mass accumulation rate.

4.2. Oceanic Observations of the Burial Efficiency of Organic Carbon

The ocean and sedimentary data from a variety of studies with emphasis on the factors affecting the efficiency of organic carbon burial was summarized by Betts and Holland (1991). They concluded that only the sedimentation rate exerted a strong effect on the carbon burial and that the oxygen content did not exert any discernible effect. We want to reanalyze these data sets.

Figure 10(A) shows the positive correlation between the burial efficiency, BE, and the sedimentation rate. The sedimentation rate is undoubtedly an important parameter based on the data set. Note, however, the high scatter in BE at high sedimentation rates. BE is defined as the fraction of the organic carbon flux at the bottom of the ocean that is actually buried in sediments. For our purposes the related quantity, the net carbon burial flux in sediments, BF_c, is of direct interest because this flux, averaged over the entire ocean, is our $F_{b,org}$, which is the net input of oxygen into the atmosphere from organic photosynthetic processes.

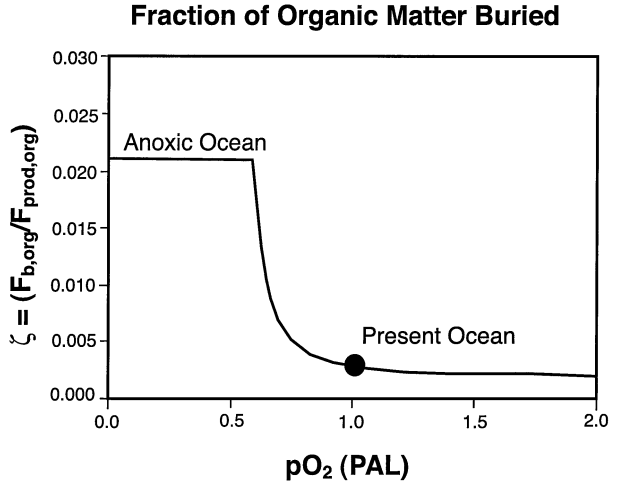

Fig. 9. Theoretical estimation of the relationship between the burial fraction of organic matter, ξ, and the atmospheric p_{O_2}. K_{O_2}, the Michaelis–Menten parameter [see Eqn. (59)], has the value 20 μM and d_{min} = 15 μM [see Eqn. (67)].

Figure 10(B) shows clearly that low sedimentation rates are associated with high $[O_2]_d$ and high sedimentation rates are associated with low $[O_2]_d$ (which may be due to a variety of factors). In fact, a strong dependence of $F_{b,org}$ on $[O_2]_d$ is seen in the data but for low values of $[O_2]_d$. However, based on the results of Fig. 10(B), this oxygen dependence in the Betts and Holland (1991) data was masked in their treatment by the scatter in the sedimentation rate. A much better approach is to include both the sedimentation rate (ω) dependence and the dependence on $[O_2]_d$ to separate their effect on the burial C flux. The sedimentation rate dependence will be assumed to be of the form ω^n as suggested by Betts and Holland (1991) and Fig. 10(A). The oxygen dependence will be obtained from the kinetic model developed in sect. 4.1. Figure 10(C) compares the combined model with the Betts and Holland (1991) data. Note that the variation in the observed data is accounted for quite nicely by including both variables and that the scatter in the respective high sedimentation rate or high $[O_2]_d$ regions is eliminated by taking into account the other variable. The overall model used in Fig. 10(C) corresponds to an equation of the form

$$\bar{F}_{b,org} = 0.003^{(f/f_{today}-1)} \left(\frac{\omega}{34}\right)^{1.26}, \qquad (68)$$

where ω is the sedimentation rate (cm/K yr) and $\bar{F}_{b,org}$ is in units of g/m^2/yr. f is defined by Eqn. (59). The factor of 34 cm/K yr is just a normalization factor, i.e., $\bar{F}_{b,org}$ = 1 g/m^2/yr for today's conditions and an average clastic sedimentation rate of 34 cm/K yr. Equation (68) is a fairly good approximation to the overall trends in the Betts and Holland (1991) data. Most importantly, because Eqn. (64) has established a very strong influence of p_{O_2} on $[O_2]_d$, Eqn. (68) documents and introduces a significant feedback between p_{O_2} and $F_{b,org}$.

In contrast to the strong ω dependence of the open sea ξ data (Betts and Holland, 1991), the Black Sea data of Arthur and Dean (1998) indicate a much lesser dependence of anoxic ξ values on ω. Based on the data in Fig. 8, the sedimentation rate dependence of anoxic ξ can be expressed as $\omega^{0.30}$. Under oxic conditions, high sedimentation rates are expected to play an important role in preventing the oxidation of organic matter traveling through the water column. It is reasonable to expect that such a role would diminish greatly under anoxic conditions.

Tim Drever, in reviewing this paper, pointed out that in using Eqn. (68), we are applying the dependence of $F_{b,org}$ on $[O_2]_d$ based on many specific localities to the "global average" flux based on an "average" $[O_2]_d$. He correctly states that the functional dependence of a quantity on an average property does not have to be the same as the average of that quantity (e.g., see Lasaga et al., 1994 for a similar discussion on global temperature). We fully agree with his statement. At this point, not introducing a full ocean dynamic model into our treatment of $F_{b,org}$, we have to use the average $[O_2]_d$ in studying the role

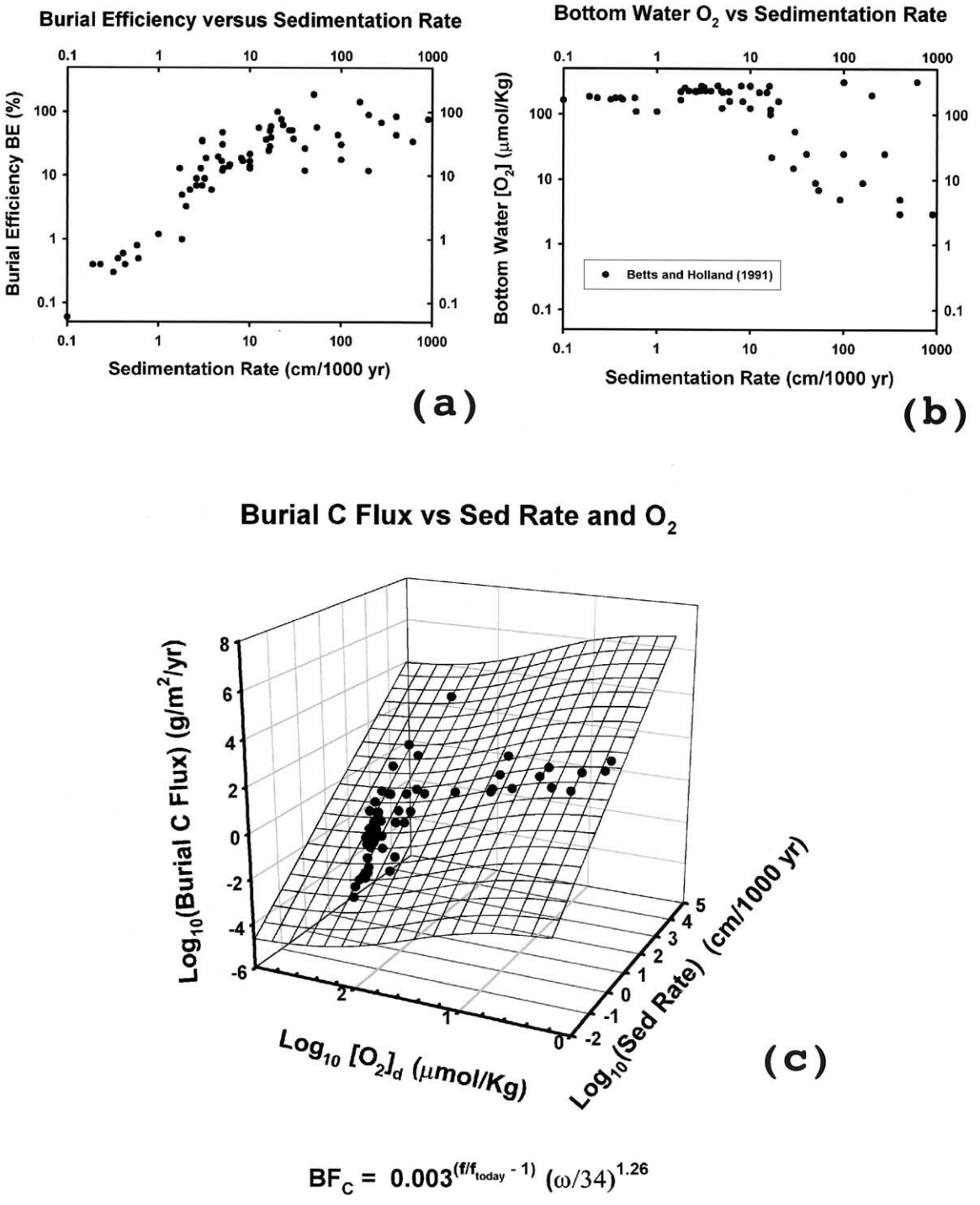

Fig. 10. (a) Relationship between the burial efficiency of organic matter (BE) and the sedimentation in modern ocean (data from Betts and Holland, 1991). BE is defined as the percentage of organic matter buried in the sediments with respect to the amounts of organic matter settled on the seafloor. (b) Relationship between the bottom water O_2 content and the sedimentation rate. (c) Comparison of the burial carbon flux data of Betts and Holland (1991) with the predictions of our model [Eqn. (68)] as a function of both ω and $[O_2]_d$.

of $F_{b,\mathrm{org}}$ on the stability and dynamics of the oxygen geochemical cycle. Nonetheless, it is an important future task to begin the process of what we would term the "statistical mechanics of global change". This task would include understanding what is required to relate average or global quantities, such as the fluxes discussed in this paper, to the underlying physical, chemical, biological and geological parameters, which are both heterogeneous on various spatial scales and variable in time.

To conclude our treatment of $F_{b,\mathrm{org}}$, the full coupled model discussed earlier will include a variety of modifications to $F_{b,\mathrm{org}}$ based on the effects due to both weathering and the oxidation of organic matter during and after burial. It is expected that the sedimentation rate will be proportional to the erosion rate of soils. Therefore,

$$\frac{w}{w^0} = \frac{dh/dt}{dh/dt^0}. \tag{69}$$

The final expression for $F_{b,\mathrm{org}}$ in the full model, then, is given by

$$F_{b,\mathrm{org}} = F^0_{b,\mathrm{org}} \left(\frac{p_{\mathrm{CO_2}}}{p^0_{\mathrm{CO_2}}}\right)^{x_{\mathrm{CO_2,org}}} \frac{A_{\mathrm{land}}}{A^0_{\mathrm{land}}} \frac{\xi}{0.003} \left[\frac{dh/dt}{dh/dt_{\mathrm{today}}}\right]^{1.26} \tag{70}$$

and under nearly anoxic conditions by

$$F_{b,\mathrm{org}} = F^0_{b,\mathrm{org}} \left(\frac{p_{\mathrm{CO_2}}}{p^0_{\mathrm{CO_2}}}\right)^{x_{\mathrm{CO_2,org}}} \frac{A_{\mathrm{land}}}{A^0_{\mathrm{land}}} 0.021 \left[\frac{dh/dt}{dh/dt_{\mathrm{today}}}\right]^{0.30} \tag{71}$$

In our calculations, the effects of sedimentation may be turned off in some cases by using an exponent of 0 instead of 1.26 or 0.30.

Given $F_{b,\mathrm{org}}$, it is of interest to calculate the total weight percent content of C in marine sediments predicted by the model. Physical erosion will contribute old detrital organic carbon into new sediments. The amount of detrital organic material and the newly formed and buried organic matter, $F_{b,\mathrm{org}}$, will jointly determine the organic matter content of recent sediments, $W_{\mathrm{sed,org}}$. The total flux of detrital material being dumped into the oceans, $F_{\mathrm{det,sed}}$, is given by

$$F_{\mathrm{det,sed}} = 10^7 \frac{dh}{dt} A_{\mathrm{land}} \rho_{\mathrm{soil}} \text{ g/K yr}. \tag{72}$$

The amount of detrital organic matter added to these sediments, $F_{\mathrm{det,org}}$, is given by

$$F_{\mathrm{det,org}} = F_{\mathrm{det,sed}} \frac{W_{s,\mathrm{org}}}{100} \text{ g/K yr}, \tag{73}$$

where $W_{s,\mathrm{org}}$ is the steady state organic C content of soils in Eqn. (40). In addition, the amount of new organic matter added to these sediments is $(12 \times 10^{12})\ F_{b,\mathrm{org}}$ in units of g/K yr. Altogether, the organic matter content of new sediments will be given by

$$W_{\mathrm{sed,org}} = \frac{F_{\mathrm{det,org}} + (12 \times 10^{12})\ F_{b,\mathrm{org}}}{F_{\mathrm{det,sed}}} 100. \tag{74}$$

5. RESULTS OF FULL COUPLED MODEL

5.1. O_2 Steady State with $F_{b,\mathrm{org}}$ Feedback

Our new evaluations of $F_{s,\mathrm{O_2}}$ and $F_{b,\mathrm{org}}$ enable us to return to the original Holland formulation of the oxygen level in the atmosphere discussed in Fig. 2. Figure 11 shows the variation of the total oxygen consumption flux ($F_{\mathrm{consump,O_2}} = F_{v,\mathrm{red}} + F_{s,\mathrm{O_2}}$) and of the O_2 production flux, $F_{b,\mathrm{org}}$, as a function of $p_{\mathrm{O_2}}$ based on our model. The fluxes are shown under different erosion rates. The other conditions for the figure are $F_{v,\mathrm{red}} = 2500 \times 10^{12}$ moles/K yr, $L_s = 3$ m, A_{land}, $= A^0_{\mathrm{land}}$, and $p_{\mathrm{CO_2}} = 1$ PAL. The intersects of the O_2 consumption and production curves define the steady-state $p_{\mathrm{O_2}}$ values. Clearly, the steady-state $p_{\mathrm{O_2}}$ value for conditions similar to today is very close to 1 PAL. Figure 11 is the quantitative extension and vindication of the original Holland formulation for the stability and dynamics of the oxygen geochemical cycle.

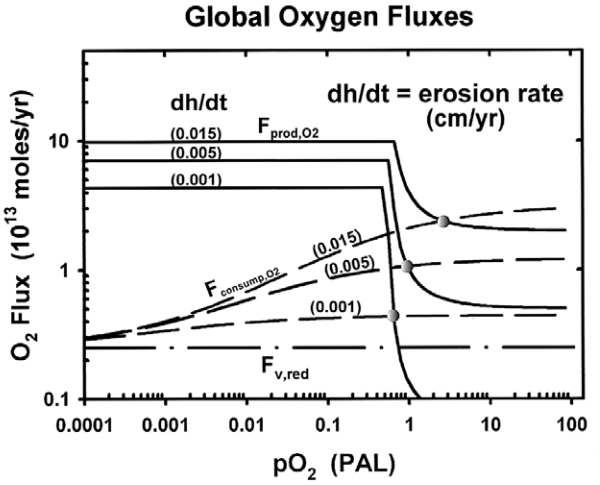

Fig. 11. Relationships between the O_2 production flux, $F_{\mathrm{prod,O_2}}$ (solid lines), and the total O_2 consumption flux, $F_{\mathrm{consump,O_2}}$ (dashed lines), versus $p_{\mathrm{O_2}}$. The other conditions are $p_{\mathrm{CO_2}} = 1$ PAL, $A_{\mathrm{land}} = A^0_{\mathrm{land}}$, and $L_s = 3$ m. $F_{\mathrm{consump,O_2}} = F_{v,\mathrm{red}} + F_{s,\mathrm{O_2}}$, where the volcanic flux of reduced gases, $F_{v,\mathrm{red}}$, is estimated to be 2500×10^{12} moles/K yr, and $F_{s,\mathrm{O_2}}$ is the O_2 consumption flux by soil fossil organic carbon. Note that the independently derived $F_{\mathrm{prod,O_2}}$ and $F_{\mathrm{consump,O_2}}$ curves for today's average erosion rate ($dh/dt = 0.005$ cm/yr) intersect at today's $p_{\mathrm{O_2}}$, and flux values.

The additional dependence of $F_{b,\mathrm{org}}$ on $p_{\mathrm{O_2}}$ modifies dramatically the steady state $p_{\mathrm{O_2}}$ calculations discussed earlier. Returning to the steady-state equation,

$$F_{s,\mathrm{O_2}} = F_{\text{net prod,O}_2} = F_{b,\mathrm{org}} - F_{v,\mathrm{redH}} - F_{v,\mathrm{red}C},$$

now the $F_{b,\mathrm{org}}$ term has a dependence on $p_{\mathrm{O_2}}$, adding an important negative feedback. This additional feedback provided by the interplay between $F_{b,\mathrm{org}}$ and $p_{\mathrm{O_2}}$, especially for low $p_{\mathrm{O_2}}$ values, can significantly affect the earlier calculations of the steady-state value of the oxygen content of the atmosphere.

Figure 12 shows the new variations of the steady-state $p_{\mathrm{O_2}}$ as a function of the erosion rate, the total input of reduced gases, $F_{v,\mathrm{red}}$, the continental land area, and the $p_{\mathrm{CO_2}}$. The term $F_{v,\mathrm{red}}$ includes both $F_{v,\mathrm{red}C}$ and $F_{v,\mathrm{red}H}$:

$$F_{v,\mathrm{red}} \equiv {}_{v,\mathrm{red}C} + F_{v,\mathrm{red}H}.$$

Figure 12(A) shows the steady state $p_{\mathrm{O_2}}$ values as a function of the soil erosion rate and the volcanic flux of reduced gases, assuming that there is no effect of sedimentation on the burial flux of organic matter (i.e., when the exponent of ω is 0). The figure shows that the steady state $p_{\mathrm{O_2}}$ value decreases with increasing rate of erosion and also with increasing flux of reduced volcanic gases. These general trends are similar to those in the system without the $F_{b,\mathrm{org}}$ feedback (see Fig. 6);

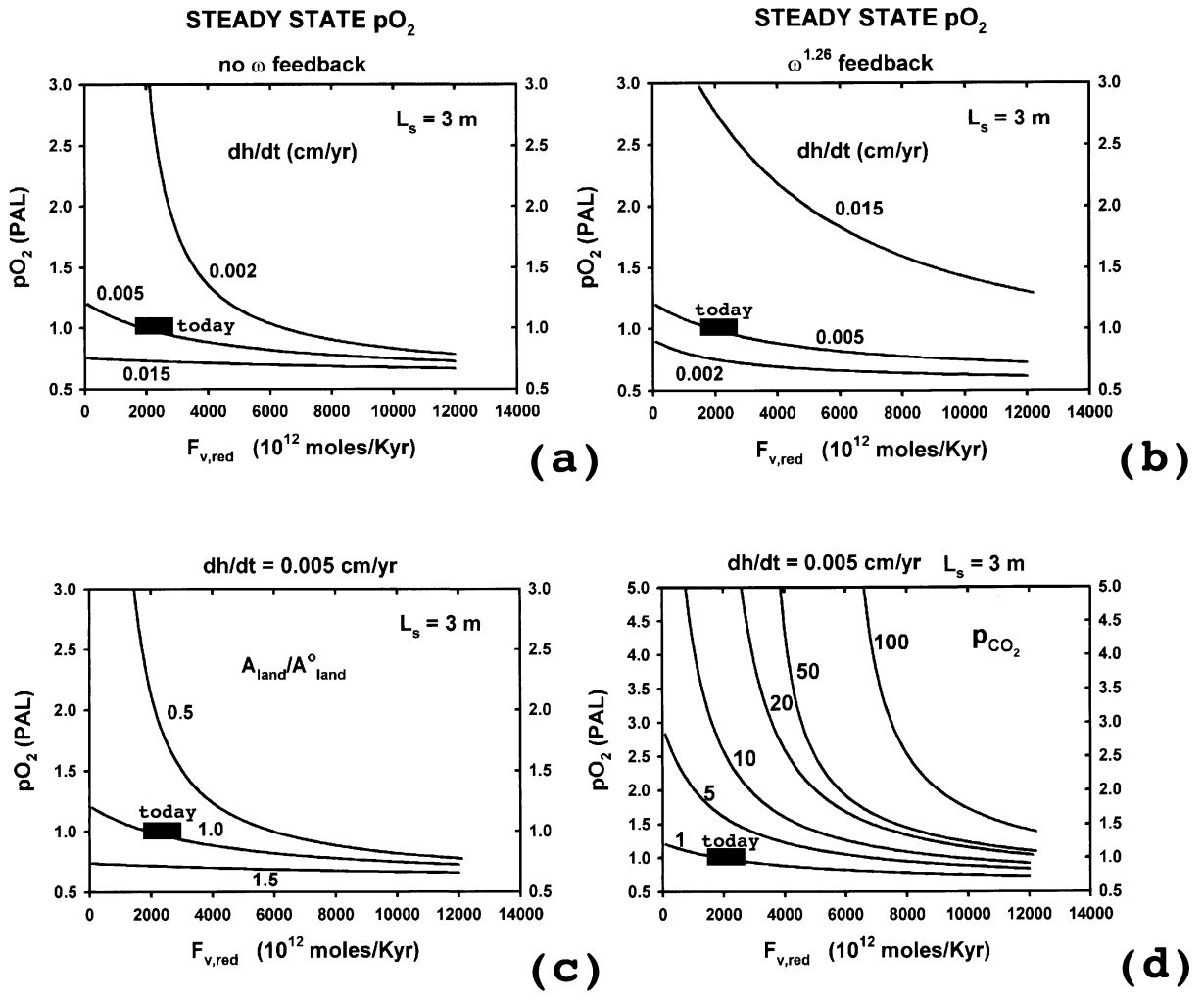

Fig. 12. The steady-state p_{O_2} values in the system with the two negative feedback mechanisms, the burial of organic C in sediments and the weathering of organic C in soils. (a) The steady-state p_{O_2} versus the flux of reduced volcanic gases (C-bearing + H-bearing) and the erosion rate with no effect of sedimentation rate on the organic burial flux. (b) The steady-state p_{O_2}, versus the flux of reduced volcanic gases (C-bearing and H-bearing) and the erosion rate with effects of sedimentation rate on the organic burial flux. (c) The steady-state p_{O_2} versus the flux of reduced volcanic gases (C-bearing and H-bearing) and the land area. (d) The steady state p_{O_2} versus the flux of reduced volcanic gases (C-bearing and H-bearing) and the p_{CO_2} values with effects of sedimentation rate on the organic burial flux.

however, the variations are much smaller. For example, the steady state p_{O_2} values vary more than 2 orders of magnitude in the C–O uncoupled system (Fig. 6), but less than 1 order of magnitude in the C–O coupled system [Fig. 12(A)]. Very low p_{O_2} levels, < 0.6 PAL, are not predicted even for very high erosion rates. Therefore, the addition of the $F_{b,org}$ feedback significantly stabilizes the oxygen content of the atmosphere.

Figure 12(B) includes the sedimentation rate effect discussed in the earlier section. Sedimentation rate feedback is strong enough to reverse the trend in the effects of erosion on p_{O_2}. Higher erosion rates now lead to higher p_{O_2} levels, reflecting the more efficient burial of organic carbon. For example, with the present flux of reduced volcanic gases (2500×10^{12} moles/K yr), an increase in the erosion rate to 3 times the present rate (i.e., $dh/dt = 0.015$ cm/yr) results in a $\sim$50% increase in p_{O_2}; a decrease in the erosion rate by 2.5 times (i.e., $dh/dt = 0.002$ cm/yr) results in a $\sim$30% decrease in p_{O_2}.

Figure 12(C) illustrates the importance of the land area, A_{land}, on the oxygen levels. A breakup of a supercontinent into smaller fragments and the distribution of them in the tropical zone with high rainfalls may significantly increase the effective total area of soil formation, A_{land}, and the erosion rate, dh/dt. On the other hand, concentrating the landmasses in the polar region with low rainfall may decrease the A_{land} and dh/dt values. Figure 12(C) shows the increase in p_{O_2} with decreasing land area. Many previous investigators (e.g., Taylor and McLennan, 1985) have suggested that the continents grew through geologic history. If the land area in the Archean was 50% of today, and if the flux of volcanic gases was the same as today, Fig. 12(C) suggests that the p_{O_2} in the Archean atmo-

sphere would have been about 2 times the present level. If the flux of reduced volcanic gases were 2 times as today and the land area one-half of today's value, the p_{O_2} value would have been roughly the same as today.

Figure 12(D) shows that the steady state p_{O_2} value increases with increasing p_{CO_2}. According to a climatic model of Kasting (1987), the p_{CO_2} of the Archean atmosphere could have been ~100 times the present level in order to compensate the lower solar flux. If so, the p_{O_2} of the Archean atmosphere could have been higher than the present level.

A change in the dynamics of the core-mantle system, such as an increased activity of mantle plumes and/or mantle convection, may change the $F_{v,red}$ value. If the Archean mantle was more reducing than today, the concentrations of reduced gases (e.g., H_2, CO, CH_4, H_2S) in Archean volcanic gases would have been higher than today's volcanic gases. In fact, some researchers (e.g., Kasting and Brown, 1998) suggest that the $F_{v,red}$ value prior to ~2 Ga was 3 to 4 times greater than today's value, resulting in an anoxic atmosphere with $p_{O_2} < 0.001$ PAL. However, the results of our computations in Fig. 12 indicate that the steady-state p_{O_2} value would have been between 0.6 PAL and ~2 PAL (i.e., and oxic atmosphere), even if the Archean $F_{v,red}$ value was as much as 7 times greater than today's value, as long as the physical erosion rate was between 0.002 to 0.025 cm/yr, the average soil thickness was between 1 and 10 m, the effective soil-forming area was between 0.3 and 2 times the present size, the p_{CO_2} was less than ~100 PAL, and p_{CO_2}, and $F_{v,red}$ were positively correlated.

5.2. Dynamics of Coupled C–O System

The dynamics of the full coupled model developed here can lead to a number of significant effects. We present here just a few cases to illustrate some of the phenomena that can take place and the kinds of inputs or variations that can cause them. These results are based on actual integration of the full equations of motion [e.g., Eqns. (5)–(8)] and do not make any steady-state assumptions for any variable.

Figure 13 shows the stability of the full system to a strong perturbation. In this scenario, the input of reduced H gases was increased to 5 times the present-day value (i.e., $F_{v,redH} = 5000 \times 10^{12}$ moles/K yr), for a period of 10 million years and then reduced to the present-day value. This large input of reduced gas results in a decrease in p_{O_2} as expected. But the p_{O_2} drop is only to ~0.6 PAL after 10 Ma; the drop is not large enough to make the entire ocean anoxic. The decrease in p_{O_2} is accompanied by a dramatic drop in p_{CO_2}, to ~less than 0.1 PAL. The decrease in p_{O_2} causes an increased burial flux of organic C; and the decrease in p_{CO_2} causes a decreased burial flux of carbonate C [see Fig. 13(b)]. In reality, such large decreases in p_{O_2} and p_{CO_2} are unlikely because a decrease in the p_{CO_2} to less than ~0.5 PAL will result in global glaciation (i.e., the Snowball Earth), which in turn will cause the cessation of the global cycles of carbon and oxygen compounds and much of the biological activity on lands and in the surface layer of the oceans. Nevertheless, the model illustrates the effects of increased flux of reduced H gases on the climate and on the global geochemical cycles of carbon and oxygen. Figure 13 also shows that, after the removal of the large input of $F_{v,redH}$, both the p_{O_2} and p_{CO_2} rebound essentially to the initial values in

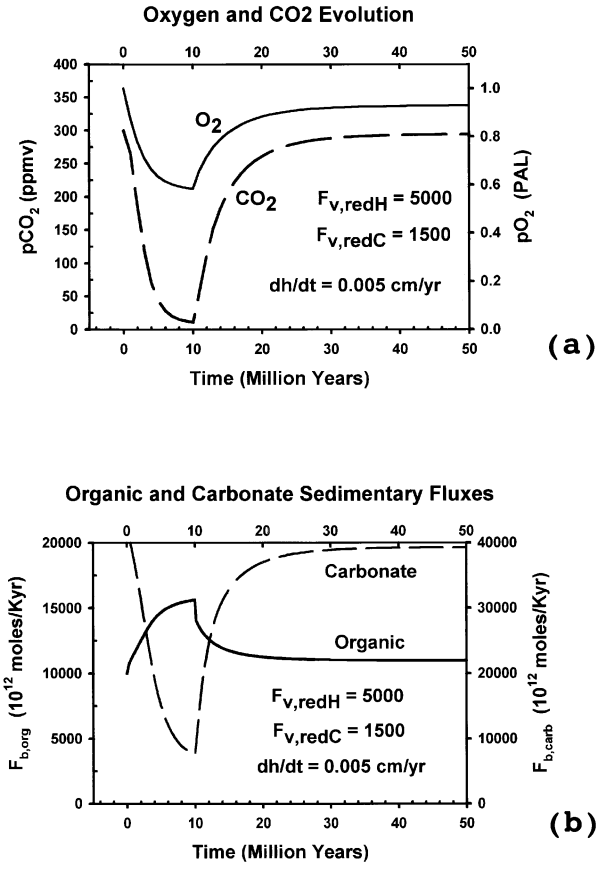

Fig. 13. Effects of a high flux of reduced H gases on the p_{O_2} and p_{CO_2} (a) and on the burial fluxes of organic C and carbonate C (b). The flux of non-C-bearing reduced volcanic gases, $F_{v,redH} = 5000 \times 10^{12}$ moles/K yr during the first 10 Ma period and $F_{v,redH} = 1000 \times 10^{12}$ moles/K yr afterward.

~10 Ma, indicating the efficiency of the two negative feedback mechanisms (the burial of organic C in sediments and the weathering of organic C in soils) to regulate the levels of atmospheric O_2 and CO_2.

6. SUMMARY

The important findings from this study are summarized below.

(1) The atmospheric oxygen level is controlled by the balance between the O_2 production flux, F_{prod,O_2} (=the burial flux of organic matter in sediments, $F_{b,org}$), and the O_2 consumption fluxes by oxidation of reduced volcanic gases, F_{v,O_2}, and by oxidation of reduced compounds (mostly organic carbon) of rocks during soil formation, F_{s,O_2}. The present flux values (in units of 10^{12} moles/K yr) are estimated to be about 10,000, 2500, and 7500 for F_{prod,O_2}, F_{v,O_2}, and F_{s,O_2}, respectively. The F_{v,O_2} value is related to the redox state of the mantle and the intensity of plate tectonics, but it is independent of the atmospheric p_{O_2} value. However, both the F_{prod,O_2} and F_{s,O_2} values are dependent on p_{O_2} as well as on various other parameters (see below).

(2) The evaluation of F_{s,O_2} is based on the experimentally determined rate law for the oxidation of coal (Chang and Berner, 1999): $F_{s,O_2} = k_+ A_{s,org} (p_{O_2})^{0.5}$ and a dynamic model for combined physical and chemical erosion in soils. The total surface area of organic carbon in the global soil system, $A_{s,org}$, is a function of p_{O_2} and of the following nine parameters.
   (i) The specific surface area of organics in the parental rocks, $\bar{A}_{s,org}$ (= 0.12 m^2/g, on average), which depends on the average grain size of the organic matter (50 × 50 × 10 μm).
   (ii)– (vi) The organic carbon content of the parental rocks, $W_{r,org}$ (= 0.44 wt. %); the densities of the organic matter (ρ_{org} = 2.26 g/cm^3), the soil (ρ_s = 2.0 g/cm^3), and the parent rock (ρ_r = 2.5 g/cm^3); the soil conversion factor ($\alpha \sim 1.4$).
   (vii) The average thickness of soil zone, L_s (1 to 10 m).
   (viii) The total land area of soil formation, A_{land} (= 1.5 × 10^{14} m^2, today).
   (ix) The physical erosion rate of soils (dh/dt = 0.005 cm/yr, today).

   The erosion rate becomes an important parameter because the organic matter in soils may or may not be completely oxidized during the average life of a soil zone (<2 Ma). Fresh organic matter is continuously added to the bottom of a soil zone as partially oxidized organic matter is removed from the top. The steady-state fossil organic C content of soils may range from 0 to 0.7 wt.%, depending on the values of the above nine parameters and p_{O_2}.

(3) Some previous investigators (e.g., Kasting, 1987; Berner, 2001) have assumed that the oxidation of organic matter is so fast that the O_2 consumption flux by soils is independent of p_{O_2} in the p_{O_2} range of interest. However, our calculations indicate that the F_{s,O_2} flux becomes independent of p_{O_2} only at extremely high p_{O_2} (>100 PAL) or extremely low erosion rates ($dh/dt < 0.0005$ cm/yr). At p_{O_2} between $\sim 10^{-5}$ and $\sim 10^{-2}$ PAL, F_{s,O_2} increases with increasing p_{O_2} and increasing erosion rate. At $p_{O_2} < \sim 10^{-5}$ PAL, the logarithm value of F_{s,O_2} increases linearly with increasing $\log(p_{O_2})$ value with a slope of 0.5 but is independent of the erosion rate. The response time for soils to attain a steady state p_{O_2} value is typically less than 10 Ma. Therefore, the strong dependence of F_{s,O_2} on p_{O_2} and the fast response time indicate that the oxidation of soil organic matter is a very effective negative feedback mechanism for regulating the atmospheric p_{O_2}.

(4) The production flux of O_2, F_{prod,O_2}, corresponds to the burial flux of organic carbon in marine sediments, $F_{b,org}$, and $F_{b,org} = \xi F_{prod,org}$, where ξ is the burial efficiency and $F_{prod,org}$ is the production flux of organic carbon in the surface oceans. The $F_{prod,org}$ value is proportional to the flux of PO_4^{3-}, an essential nutrient, to the surface oceans. The PO_4^{3-} flux depends on the atmospheric p_{CO_2} and on the total land area. Betts and Holland (1991) conclude that the ξ value strongly depends on the clastic sedimentation rate, ω, but only weakly dependent on the dissolved O_2 content of the deep oceans, $[O_2]_d$. However, our theoretical analysis of the oxidation kinetics of organic matter by organisms and our analyses of organic carbon contents of marine sediments suggest a very strong dependency of ξ on both $[O_2]_d$ and ω. The ξ increases from 0.003 in the normal modern oceans to 0.021 in anoxic oceans. The $[O_2]_d$ value can be related to the dissolved O_2 content of the high latitude shallow ocean, $[O_2]_h$, which depends on the atmospheric p_{O_2} and the solubility constant; the C/P ratio of the buried organic carbon (= 172 today), and the difference in the phosphate contents between the shallow and deep ocean waters. For example, the deep ocean becomes anoxic ($[O_2]_d = 0$) at $p_{O_2} \leq 0.51$ PAL. Therefore, the production flux of O_2 at $p_{O_2} < 0.51$ PAL will become about 7 times higher than that at 1 PAL. The strong dependency of $F_{b,org}$ on p_{O_2} is another important negative feedback mechanism for regulating the atmospheric p_{O_2}.

(5) In a system with the two negative feedback mechanisms, the steady-state p_{O_2} value decreases with decreasing erosion rate (dh/dt), with increasing land area of soil formation (A_{land}), with increasing flux of reduced volcanic gas ($F_{v,red}$), and with decreasing atmospheric CO_2 level (p_{CO_2}). For the likely ranges of these parameters since the Paleoproterozoic time, the atmospheric p_{O_2} level is likely to have stayed within a very narrow range of 0.6–2 PAL, indicating the stability of the oxygenated atmosphere. If the atmospheric p_{O_2} level can fluctuate significantly and can drop below about 0.5 PAL, the deep ocean water will probably become anoxic (e.g., Sarmiento, 1992), causing extinction of most eukaryotic organisms, including animals and plants, in deep oceans; the ozone shield in the atmosphere will also become considerably thinner, causing extinction of most land-based organisms. However, our study suggests that both the low p_{O_2} atmosphere ($p_{O_2} < 0.5$ PAL) and the very high p_{O_2} atmosphere ($p_{O_2} > 2$ PAL) are unstable. Thus, either is an unlikely scenario in geologic history when photosynthetic organisms (e.g., cyanobaeteria) are the primary producers of organic matter in the oceans.

(6) The results of our calculations are also consistent with and provide kinetic and quantitative justification for the lack of large p_{O_2} variations during the last 540 M yr period based on the sulfur and carbon isotope records of Phanerozoic sedimentary rocks (e.g., Lasaga, 1989; Berner et al., 2000; Berner, 2001).

Acknowledgments—The authors are indebted to Yumiko Watanabe for helpful assistance in preparation of the paper. Valuable discussion was provided by Hu Barnes, Ken Towe, Mike Arthur, Andy Kurtz, Shuhei Ono, and Kosei Yamaguchi. In addition, Tim Drever significantly improved an earlier version of the paper. The authors would like to gratefully acknowledge financial support from Department of Energy Grant No. DE-FG02-90ER14153, National Science Foundation Grants Nos. EAR-9628238 and EAR-9529258 to Lasaga, and from NASA Astrobiology Program (NCC2-1057), NASA Exobiology Program (NAG5-9089), and NSF (EAR-9706279) to Ohmoto.

Associated editor: M. S. Ghiorso

REFERENCES

Arthur M. A., Dean W. E., Neff E. D., Hay B. J., King J., and Jones G. (1994) Varve calibrated records of carbonate and organic carbon accumulation over the last 2000 years in the Black Sea. *Global Biogeochem. Cycles* **8,** 195–217.

Arthur M. A. and Dean W. E. (1998) Organic-matter production and preservation and evolution of anoxia in the Holocene Black Sea. *Paleoceanography* **13,** 395–411.

Berner R. A. (1980) *Early Diagenesis: A Theoretical Approach*, Princeton University Press.
Berner R. A. (1991) A model for atmospheric CO_2 over Phanerozoic time. *Am. J. Sci.* **291,** 339–376.
Berner R. A. (1999) A new look at the long-term carbon cycle. *GSA Today*, November, 2–6.
Berner R. A. (2001) Modeling atmospheric O_2 over Phanerozoic time. *Geochim. Cosmochim. Acta* **65,** 685–694.
Berner R. A., Lasaga A. C., and Garrels R. M. (1983) The carbonate–silicate geochemical cycle and its effect on atmospheric carbon dioxide over the past 100 million years. *Am. J. Sci.* **283,** 641–683.
Berner R. A., Petsch S. T., Lake T. A., Beerling D. J., Popp B. N., Lane R. S., Laws E. A., Westley M. B., Cassar N., Woodward F. I., and Quick W. P. (2000) Isotope fractionation and atmospheric oxygen: Implications for Phanerozoic O_2 evolution. *Science* **287,** 1630–1633.
Betts J. N. and Holland H. D. (1991) The oxygen content of ocean bottom waters, the burial efficiency of organic carbon, and the regulation of atmospheric oxygen. *Palaeogeography, Palaeoclimatology, Palaeoecology* **97,** 5–18.
Boudreau B. P. and Westrich J. T. (1984) The dependence of bacterial sulfate reduction on sulfate concentration in marine sediments, *Geochim. Cosmochim. Acta* **48,** 2503–2516.
Brady P. V. (1991) The effect of silicate weathering on global temperature and atmospheric CO_2. *J. Geophys. Res.* **96,** 18101–18106.
Carroll D. (1970) *Rock Weathering.* Plenum.
Chang S. and Berner R. A. (1999) Coal weathering and the geochemical carbon cycle. *Geochim. Cosmochim. Acta* **63,** 3301–3310.
Drever J. I. (1997) *The Geochemistry of Natural Waters.* Prentice Hall.
Garrels R. M. and Lerman A. (1984) Coupling of the sedimentary sulfur and carbon cycles—an improved model. *Am. J. Sci.* **284,** 989–1007.
Holland H. D. (1973) Ocean water, nutrients and atmospheric oxygen. In *Proceedings of Symposium on Hydrogeochemistry and Biochemistry* (ed. E. Ingerson), pp. 68–81. Clarke.
Holland H. D. (1978) *The Chemistry of the Atmosphere and Oceans.* Wiley.
Holland H. D. (1984) *The Chemical Evolution of the Atmosphere and Oceans.* Princeton University Press.
Holland H. D. (1994) Early Proterozoic atmospheric change. In *Early Life on Earth* (ed. S. Bengtson), pp. 237–244. Columbia University Press.
Holland H. D. (1999) When did the Earth's atmosphere become oxic? A Reply. *Geochem. News* **100,** 20–22.
Jahnke L. and Klein H. P. (1979) Effects of low levels of oxygen on Sacchromyces cerevisial. *Origins of Life* **9,** 329–334.
Kasting J. F. (1987) Theoretical constraints on oxygen and carbon dioxide concentrations in the Precambrian atmosphere. *Precambrian Res.* **34,** 205–229.
Kasting J. F. and Brown L. L. (1998) The early atmosphere as a source of biogenic compounds. In *Molecular Origins of Life* (ed. A. Brack), pp. 35–56. Cambridge University Press.
Knoll A. H. (1992) The early evolution of eukaryotes: a geological perspective. *Science* **256,** 622–627.
Kump L. R. (1988) Terrestial feedback in atmospheric oxygen regulation by fire and phosphorus. *Nature* **335,** 152–154.
Kump L. R. and Garrels R. M. (1986) Modeling atmospheric O_2 in the global sedimentary redox cycle. *Am. J. Sci.* **286,** 337–360.
Kump L. R. and Arthur M. A. (1999) Interpreting carbon–isotope excursions: carbonates and organic matter. *Chem. Geol.* **161,** 181–198.
Lasaga A. C. (1989) A new approach to isotopic modeling of the variation of atmospheric oxygen through the phanerozoic. *Am. J. Sci.* **289,** 411–435.
Lasaga A. C. (1998) *Kinetic Theory in the Earth Sciences.* Princeton University Press.
Lasaga A. C., Berner R. A., and Garrels R. M. (1985) An improved geochemical model of atmospheric CO_2 fluctuations over the past 100 million years. In *The Carbon Cycle and Atmospheric CO_2: Natural Variations Archean to Present* (eds. E. Sundquist and W. S. Broecker) *Geophysical Monograph* **32,** 397–411.
Lasaga A. C., Soler J. M., Ganor J., Burch T. E., Nagy K. L. (1994) Chemical Weathering rate laws and global geochemical cycles. *Geochim. Cosmochim. Acta* **58,** 2361–2386.
Lenton T. M. and Watson A. J. (2000) Redfield revisited 2. What regulates the oxygen content or the atmosphere? *Global Biogeochem. Cycles* **16,** 249–268.
Ohmoto H. (1997) When did the Earth's atmosphere become oxic? *Geochem. News* **93,** 26–27.
Sarmiento J. and Toggweiler J. R. (1984) A new model for the role of the oceans in determining atmospheric p_{CO_2}. *Nature* **308,** 621–624.
Sarmiento J. (1992) Biogeochemical Ocean Models. In *Climate System Modeling* (ed. K. E. Trenberth), pp. 519–564. Cambridge University Press.
Schopf J. W. (1994) The oldest known records of life: early Archean stromatolites, microfossils, and organic matter. In Bengtson, S., ed., *Early Life on Earth* (ed. S. Bengtson), pp. 193–206. Columbia University Press.
Sundquist E. T. (1985) Geological perspective on carbon dioxide and the carbon cycle. In *The Carbon Cycle and Atmospheric CO_2: Natural Variations, Archean to Present*, (eds. E. T. Sundquist and W. S. Broecker), pp. 5–59. AGU.
Taylor S. R. and McLennan S. M. (1985) *The Continental Crust: Its Composition and Evolution.* Blackwell Scientific.
Van Cappellen P. and Ingall E. D. (1996) Redox stabilization of the atmosphere and oceans by phosphorus-limited marine productivity. *Science* **271,** 493–496.
Watanabe Y., Naraoka H., Wronkiewics D. J., Condie K. C., and Ohmoto H. (1997) Carbon, nitrogen, and sulfur geochemistry of Archean and Proterozoic shales from tile Kaapvaal Craton, South Africa. *Geochim. Cosmochim. Acta* **61,** 3441–3459.
Watson A. J., Lovelock J. E., and Margulis L. (1978) Methanogenesis, fires and the regulation of atmospheric oxygen. *Biosystems* **10,** 293–298.

APPENDIX

The dependence of the experimental rate of oxidation of coal on the square root of the oxygen concentration is a significant result. As such, it is important to justify the rate law based on what is known from surface chemical kinetics. Figure 14 gives a probable mechanism that accounts for the square-root dependence of the rate. The first step involves molecular adsorption of the O_2 molecule on the organic surface. The adsorbed O_2 molecules can then use the organic substrate to dissociate into adsorbed oxygen atoms [step (2)]. Such dissociation has been commonly observed with diatomic molecules on solid surfaces (Lasaga, 1998). These adsorbed oxygen atoms can also recombine to form adsorbed oxygen molecules, thereby leading to an equilibrium relationship [step (2)]. The slow step in the oxidation involves the cleavage of the carbon–carbon bonds and the formation of CO by the reactive adsorbed oxygen atoms [step (3)]. The CO products are quickly oxidized to CO_2 [step (4)]. The rate-determining step is proportional to the concentration of adsorbed oxygen atoms [Eqn. (A1)]. But from the previous equilibrium relationship between adsorbed oxygen molecules and adsorbed oxygen atoms [step (2)], the concentration of adsorbed oxygen atoms is proportional to the square root of the adsorbed oxygen molecules [Eqn. (A2)]. If the adsorbed oxygen molecules are linearly related to the amount of oxygen in the fluid, the overall rate has a square-root dependence on p_{O_2} [Eqn. A3)]. Such square-root dependencies have been observed in other heterogeneous reaction mechanisms (e.g., Lasaga, 1998). We add the possible mechanism here because it has not been presented in this regard by Chang and Berner (1999). Note that the mechanism proposed for the experimental data is independent of any bacterial action. Also note that the mechanism would apply even if some of the intermediate oxidation products are complex humic substances, as observed in part by Chang and Berner. Finally, the mechanism assumes that the oxygen molecules obey a linear adsorption isotherm, which is consistent with other studies of neutral diatomics on crystal surfaces (Lasaga, 1998).

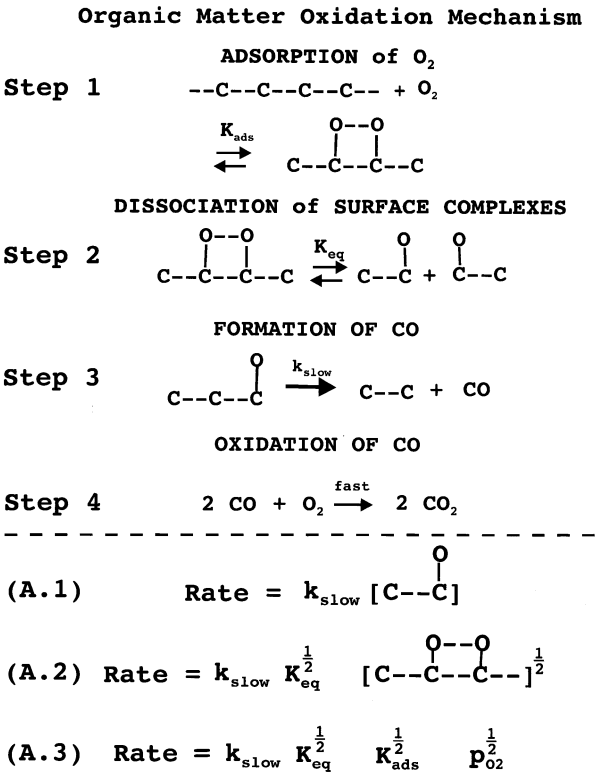

Fig. 14. The proposed reaction mechanism for the oxidation of coal and kerogen by molecular oxygen.